Single-spin asymmetries in muon pair production

Robert D. Carlitz and Raymond S. Willey
Department of Physics and Astronomy, University of Pittsburgh, Pittsburgh, Pennsylvania 15260
(Received 7 August 1991)

Theoretical analyses of polarized leptoproduction data suggest that the polarized gluon structure function might be large, but there has been no independent measurement of this quantity. Measurements of single-spin asymmetries in the production of muon pairs from the scattering of two protons, one of which is longitudinally polarized, can be interpreted in terms of polarized gluon, quark, and antiquark structure functions. We develop this interpretation in detail and compute the size of the asymmetries that might be expected for this process.

PACS number(s): 13.88.+e, 12.38.Bx, 12.38.Qk, 13.85.Qk

I. INTRODUCTION

Polarized leptoproduction experiments [1, 2] have shown that a polarized proton has an interesting spin substructure. Quarks carrying a large fraction of a longitudinally polarized proton's momentum are found to be highly polarized. The degree of polarization varies with the longitudinal momentum fraction and differs for different flavors of quarks. Recent experiments [2] have shown that the simple assumption [3, 4] that only up and down quarks should carry the proton's spin cannot be correct. This suggests that either the strange quarks should carry a significant fraction of the proton's spin or that the gluons within the proton should be highly polarized [5].

The first alternative might seem improbable [6], since it would require the strange quarks in the proton to be highly polarized down to rather small values of the longitudinal momentum fraction x. The second alternative might also seem improbable since it would require [7] the gluons to be highly polarized down to small values of x, but there is no data which directly contradicts this idea. Furthermore, the expectations of quantum chromodynamics (QCD) [8] are that the gluon spin fraction should grow indefinitely as one increases the momentum scale on which one probes the proton's structure. (A gluon spin fraction greater than 1 is accommodated in QCD by a large and oppositely oriented component of orbital angular momentum.)

High-energy hadron colliders offer the possibility of exploring partons at increasingly small longitudinal momentum fractions for a given value of the transverse momentum (or partonic scale). At these small momentum fractions the parton densities become large, either through the mechanism of gluon bremsstrahlung as embodied in the evolution equations of Altarelli and Parisi [10] or through an intrinsic component associated [9] with the structure of the Pomeron in QCD. In this sense new hadron colliders provide gluon beams of high intensity. From the viewpoint of the strong interactions, then, the question of whether these colliders should accommodate polarized beams is simply a question of whether these gluons would be highly polarized.

We see that one's interpretation of current leptoproduction data may have an important influence on the design of new hadron colliders. For this reason—and for a better understanding of the substructure of the polarized proton—it is important to resolve the question of whether the gluons in a polarized proton are themselves highly polarized. This is not a question which can be resolved from inclusive leptoproduction data alone. Indeed the first moment of the polarized structure function can always be written as a sum of terms

$$\int G_1(x,q^2)dx = \tfrac{4}{9}\Delta u' + \tfrac{1}{9}\Delta d' + \tfrac{1}{9}\Delta s'. \tag{1.1}$$

Each of these terms corresponds to a matrix element of a component of the axial vector current, e.g.,

$$< p,s|\bar{u}\gamma_\mu\gamma_5 u|p,s >= s_\mu(p)\Delta u'. \tag{1.2}$$

Within the context of leptoproduction data there is no way to distinguish between the naive interpretation, which identifies $\Delta u'$ with the spin fraction carried by the up quark, and an interpretation [5] which identifies $\Delta u'$ as

$$\Delta u' = \Delta u - (\alpha_S/2\pi)\Delta G. \tag{1.3}$$

Here Δu denotes the spin fraction carried by the up quark and ΔG the gluon spin fraction, which enters the matrix element of the axial vector current (1.2) as a consequence of the axial anomaly.

If one wishes to isolate the up-quark and gluon contributions to (1.3) separately, it is necessary to examine experimental quantities which are directly sensitive to the gluon spin fraction—quantities for which ΔG does not have the formal structure of a higher-order correction to Δu. If ΔG makes a contribution of any significance to Eq. (1.3), then its contribution to these other processes will be extremely large, since the relative suppression factor of $\alpha_S/2\pi$ will no longer be present. This makes an experimental search for ΔG much easier to undertake.

Unfortunately the experimental situation is by no means simple or obvious. Experiments which require polarized beams and targets are technically difficult, long,

and expensive. In leptoproduction experiments it is possible to separate the quark and gluon contributions to the g_1 if one identifies [11] one or two hadronic jets in the final state. The single-jet events correspond to quark-initiated processes; two-jet events are either radiative corrections to these quark-initiated processes or gluon-initiated processes. The latter are dominant for large-transverse-momentum jets. This is not a simple experiment to carry out. The optimal facility for such a measurement might be a lepton-hadron collider such as the DESY e-p collider HERA, but HERA lacks any provision for a polarized proton beam.

The availability of high-energy colliders with polarized proton beams would allow one to carry out a number of experiments [7, 12] which are sensitive to the polarized gluon component of the proton. No such machines exist at present, although an option of this sort exists for the BNL Relativistic Heavy Ion Collider (RHIC). The upgrade of any present hadron collider to accommodate polarized beams seems unlikely at present. Hence one would have to work with extracted tertiary beams and external polarized targets. The massive effort for such an experimental program also makes it unlikely at present.

This leaves the possibility of using processes for which only a polarized beam or a polarized target would be required. Measurements of the "single-spin asymmetries" that might be detected in such an experiment form the subject of the present paper. We consider the specific process

$$p^{\uparrow} + p \rightarrow \mu^+ + \mu^- + X \tag{1.4}$$

as typical and as a process which should be relatively easy to examine experimentally. The required experimental setup would involve either an extracted (unpolarized) beam and a polarized external target or an (unpolarized) internal beam and a polarized internal storage cell [13].

If one is interested in finding asymmetries for longitudinally polarized protons, and if one is dealing with a parity-conserving amplitude, then it is necessary to measure the momentum of at least two particles in the final state. Indeed, the spin vector for the polarized proton in the initial state must be correlated with some axial vector defined by the various measured momentum vectors. If only one particle is measured in the final state, then the only such axial vector would be the normal to the plane defined by this momentum and the collision axis of the incident particles, and the only possible asymmetry would have to involve transverse components of the initial spin vector. If the momenta of two particles are measured in the final state, then their cross product defines an axial vector which can have a longitudinal component. For the process (1.4) these two momenta are the momenta $\mathbf{q}^+$ and $\mathbf{q}^-$ of the μ^+ and μ^- particles. The transverse momentum of the pair,

$$Q_\perp = q_\perp^+ + q_\perp^-, \tag{1.5}$$

must also be nonzero for the longitudinal spin asymmetry to be nonvanishing (since otherwise $\mathbf{q}^+ \times \mathbf{q}^-$ would have no longitudinal component).

The longitudinal spin asymmetry for the process (1.4) is proportional to the quantity $\mathbf{s}\cdot\mathbf{q}^+ \times \mathbf{q}^-$, where $\mathbf{s}$ denotes the proton's spin. This quantity is odd under time reversal. Hence the asymmetry must arise from the imaginary part of the muon pair production amplitude. It follows that there is no asymmetry at the tree level in quantum chromodynamics, and that the asymmetry at order α_S is determined by the structure of one-loop contributions to the production amplitude. In essence, the goal of this paper will be to calculate the coefficients of α_S that occur in the various partonic subprocesses that contribute to the hadronic process (1.4). If these coefficients are not small, then it should be practical to measure the polarization asymmetry for moderate values of Q^2, say $Q^2 \sim 10$–25 GeV^2.

We find this to be the case and identify the regions of phase space where the contributing parton subprocesses have relatively large asymmetries. These results indicate that experiments which focus upon the process (1.4) should be feasible to carry out and should provide significant data on the magnitude of the gluon spin component of the proton. We feel [14] that these experiments may offer the best way of obtaining this information with the use of any existing particle accelerators.

The following two parton subprocesses and their charge conjugates contribute to muon pair production:

$$q + \bar{q} \rightarrow \mu^+\mu^- + G, \tag{1.6}$$

$$G + q \rightarrow \mu^+\mu^- + q. \tag{1.7}$$

A third process,

$$G + G \rightarrow \mu^+\mu^- + q + \bar{q}, \tag{1.8}$$

can also contribute to muon pair production, but this process is of higher order in perturbative QCD than either of the processes (1.6) and (1.7) and is thus relatively less important at large Q^2. In the present paper we shall only discuss the contributions of the leading-order processes, (1.6) and (1.7). In the next section of this paper we discuss the kinematics common to these two process. In Sec. III we discuss the process (1.6) in detail, considering both the unpolarized cross section and the cross sections for polarized quarks or antiquarks. In Sec. IV we consider the gluon-quark process and evaluate the associated single-spin asymmetries for this process. Section V discusses the relevance of these parton processes in proton-proton scattering experiments. Section VI summarizes our results, discusses their consequences for experiment, and lists related processes which might be considered in a similar vein. Details of the calculations of Secs. III and IV may be found in Appendix A and a set of tables. In Appendix B we discuss the relation of the current work to previously published results.

II. KINEMATICS

The parton-level kinematics are the same for any of the processes that we will discuss in this paper. In each case two incident partons collide to produce a virtual photon and an outgoing parton. The incident partons arise from each of the colliding hadrons, the virtual photon decays into a $\mu^+\mu^-$ pair, and the outgoing parton materializes

as a hadronic jet. We label the momenta of the incident partons by p_1 and p_2; Q denotes the momentum of the virtual photon, and K the momentum of the outgoing parton or jet. The individual muons have momenta q^+ and q^-, but it will frequently be more convenient to use the linear combinations

$$Q_\mu = q_\mu^- + q_\mu^+, \tag{2.1}$$

$$q_\mu = q_\mu^- - q_\mu^+. \tag{2.2}$$

If $Q^2 \gg m_\mu^2$, we can ignore the muon mass m_μ and use the approximations

$$q \cdot Q \simeq 0, \tag{2.3}$$

$$q^2 \simeq -Q^2. \tag{2.4}$$

We will denote the invariant momenta formed from the parton variables by

$$\hat{s} = (p_1 + p_2)^2, \tag{2.5}$$

$$\hat{t} = (K - p_2)^2 = (Q - p_1)^2, \tag{2.6}$$

$$\hat{u} = (K - p_1)^2 = (Q - p_2)^2. \tag{2.7}$$

In the center of momentum of the parton scattering process the parton momenta have the explicit forms

$$p_1^\mu = (P, 0, 0, P), \tag{2.8}$$

$$p_2^\mu = (P, 0, 0, -P), \tag{2.9}$$

$$Q^\mu = (E', q' \sin\theta, 0, q' \cos\theta), \tag{2.10}$$

$$q^\mu = (q' \cos\alpha, Q \sin\alpha \cos\beta \cos\theta + E' \cos\alpha \sin\theta, Q \sin\alpha \sin\beta, E' \cos\alpha \cos\theta - Q \sin\alpha \cos\beta \sin\theta), \tag{2.11}$$

with

$$P = \frac{1}{2}\sqrt{s}, \tag{2.12}$$

$$E' = \frac{s + Q^2}{2\sqrt{s}}, \tag{2.13}$$

$$q' = \frac{s - Q^2}{2\sqrt{s}}. \tag{2.14}$$

Equations (2.8)–(2.11) display the components of each vector in the form $x^\mu = (t, x, y, z)$. The momenta of the incident partons thus define the z axis, while the direction of the virtual photon defines the x-z plane. The angles α and β describe the decay of the virtual photon relative to these axes in the rest frame of the photon [where, according to Eq. (2.3), $q^0 = 0$]. The phase space for the decay of the virtual photon has the form

$$\frac{1}{(2\pi)^2}\frac{d^3q^+}{2q_0^+}\frac{d^3q^-}{2q_0^-}\delta^4(q^+ + q^- - Q) = \frac{1}{8(2\pi)^2}d\Omega(\alpha,\beta) = \frac{1}{8(2\pi)^2}\sin\alpha d\alpha\, d\beta. \tag{2.15}$$

We will denote the signs of the helicities of the incident partons by s_1 and s_2 and the sign of the helicity of the outgoing parton by s. Thus s has the values ± 1 for an outgoing quark of helicity $\pm\frac{1}{2}$. If the outgoing parton is a gluon, the values $s = \pm 1$ refer to helicities ± 1. The corresponding symbols for the lepton helicities are $s^\pm$. If one does not observe the spin orientations of any of the produced particles, then the parton cross section has the form

$$d\hat{\sigma} = \frac{1}{2\hat{s}Q^4}\frac{\alpha_{\rm EM}^2}{2\pi^3}\frac{d^3q^+}{2q_0^+}\frac{d^3q^-}{2q_0^-}\frac{d^3K}{2K_0} \times \delta^4(q^+ + q^- + K - p_1 - p_2)W^{\mu\nu}(s_1, s_2)L_{\mu\nu}. \tag{2.16}$$

The tensors $W^{\mu\nu}$ and $L_{\mu\nu}$ are constructed from hadron and lepton variables, respectively. If the produced muons are relativistic, then one can ignore the muon mass and write

$$L_{\mu\nu} = 2(Q_\mu Q_\nu - g_{\mu\nu}Q^2 - q_\mu q_\nu). \tag{2.17}$$

Equation (2.16) applies to the annihilation of partons with helicities of signs s_1 and s_2. If the initial particles are unpolarized, or if only one of them is polarized, then one must construct appropriate spin averages of the quantity $W^{\mu\nu}(s_1, s_2)L_{\mu\nu}$.

Of particular interest in this paper is the case where one of the initial partons is polarized, with $s_i = \pm 1$. We will designate the differential cross section for this process by $d\hat{\sigma}_\pm$. The unpolarized cross section is given by $(d\hat{\sigma}_+ + d\hat{\sigma}_-)/2$ and is obtained by replacing the factor $W^{\mu\nu}(s_1, s_2)L_{\mu\nu}$ in Eq. (2.16) by an average over initial spin orientations $\frac{1}{4}\sum_{s_1,s_2} W^{\mu\nu}(s_1, s_2)L_{\mu\nu}$. Similarly, we can construct a cross section difference $d\hat{\sigma}_+ - d\hat{\sigma}_-$ if we replace the factor $W^{\mu\nu}(s_1, s_2)L_{\mu\nu}$ in Eq. (2.16) by the quantity

$$\Delta W = \frac{1}{2}\sum_{s_1,s_2} s_i W^{\mu\nu}(s_1, s_2)L_{\mu\nu}. \tag{2.18}$$

The ratio

$$\mathcal{A} = \frac{d\hat{\sigma}_+ - d\hat{\sigma}_-}{d\hat{\sigma}_+ + d\hat{\sigma}_-} \tag{2.19}$$

defines the single-spin asymmetry that we seek to describe in this paper. In terms of the quantities just discussed this asymmetry has the form

$$\mathcal{A} = \frac{\Delta W}{\frac{1}{2}\sum_{s_1,s_2} W^{\mu\nu}(s_1, s_2)L_{\mu\nu}}. \tag{2.20}$$

We will denote by $\Delta W^{[j]}$ the contribution to ΔW of a given Feynman graph, j. Each such contribution may be written in the form

$$\Delta W^{[j]} = \frac{-e_i^2 g^4 C^{[j]}}{\pi}(A_1^{[j]} q \cdot p_1 + A_2^{[j]} q \cdot p_2) \times \epsilon_{\mu\nu\rho\sigma} p_1^\mu p_2^\nu Q^\rho q^\sigma, \tag{2.21}$$

which involves a color coefficient $C^{[j]}$ and two invariant functions $A_1^{[j]}$ and $A_2^{[j]}$. The totally antisymmetric tensor $\epsilon_{\mu\nu\rho\sigma}$ is defined to have

$$\epsilon_{0123} = +1. \tag{2.22}$$

The common factor g in Eq. (2.21) refers to the strong

coupling (with $g^2/4\pi = \alpha_S$), while e_i denotes the charge of the participating quark in units of e, the proton's charge.

It is convenient to reexpress the functions $A_1^{[j]}$ and $A_2^{[j]}$ in terms of other invariant functions [15] $T_{2,-1}^{[j]}$ and $T_{2,-2}^{[j]}$. These functions are defined by a decomposition

$$\Delta W^{[j]} = \frac{-e_i^2 g^4 C^{[j]}}{2\pi}(T_{2,-1}^{[j]} q\cdot Z + T_{2,-2}^{[j]} q\cdot X) \times \epsilon_{\mu\nu\rho\sigma} p_1^\mu p_2^\nu Q^\rho q^\sigma . \tag{2.23}$$

The vectors Z and X are an orthogonal pair of spacelike vectors each of which is orthogonal to the vector Q. In the parton center-of-momentum frame Z lies along the direction of the incident particles, while X and Z define the scattering plane for the process $q + \bar{q} \to \gamma^* + G$. Thus Z is constructed from the momenta of the incident partons, while X involves these momenta and the momentum Q. The explicit forms of Z and X are

$$Z_\mu = (Q^2 - \hat{u})p_{1\mu} - (Q^2 - \hat{t})p_{2\mu}, \tag{2.24}$$

$$X_\mu = (Q^2 - \hat{u})p_{1\mu} + (Q^2 - \hat{t})p_{2\mu} - (Q^2 - \hat{t})(Q^2 - \hat{u})Q_\mu/Q^2. \tag{2.25}$$

The relation of the functions $T_{2,-1}$ and $T_{2,-2}$ to A_1 and A_2 is given by

$$T_{2,-1} = A_1/(Q^2 - \hat{u}) - A_2/(Q^2 - \hat{t}), \tag{2.26}$$

$$T_{2,-2} = A_1/(Q^2 - \hat{u}) + A_2/(Q^2 - \hat{t}). \tag{2.27}$$

In terms of the angles α and β which characterize the lepton momenta in the rest frame of the virtual photon, the dot products $q\cdot p_1$ and $q\cdot p_2$ have the explicit forms

$$q\cdot p_1 = \frac{Q^2\hat{u} - \hat{s}\hat{t}}{2(\hat{s} - Q^2)}\cos\alpha + \frac{\sqrt{Q^2\hat{s}\hat{t}\hat{u}}}{\hat{s} - Q^2}\sin\alpha\cos\beta, \tag{2.28}$$

$$q\cdot p_2 = \frac{Q^2\hat{t} - \hat{s}\hat{u}}{2(\hat{s} - Q^2)}\cos\alpha - \frac{\sqrt{Q^2\hat{s}\hat{t}\hat{u}}}{\hat{s} - Q^2}\sin\alpha\cos\beta. \tag{2.29}$$

Hence the products $q\cdot Z$ and $q\cdot X$ in Eq. (2.23) may be written

$$q\cdot Z = \frac{Q^2\hat{s}(\hat{u} - \hat{t})}{\hat{s} - Q^2}\cos\alpha + \frac{\hat{s} + Q^2}{\hat{s} - Q^2}\sqrt{Q^2\hat{s}\hat{t}\hat{u}}\sin\alpha\cos\beta, \tag{2.30}$$

$$q\cdot X = \left(\frac{\hat{s} + Q^2}{\hat{s} - Q^2}\right)\hat{t}\hat{u}\cos\alpha + \frac{\hat{t} - \hat{u}}{\hat{s} - Q^2}\sqrt{Q^2\hat{s}\hat{t}\hat{u}}\sin\alpha\cos\beta, \tag{2.31}$$

while the cross product which appears in Eq. (2.23) can be written as

$$\epsilon_{\mu\nu\rho\sigma} p_1^\mu p_2^\nu Q^\rho q^\sigma = \frac{-1}{2}\sqrt{Q^2\hat{s}\hat{t}\hat{u}}\sin\alpha\sin\beta. \tag{2.32}$$

Owing to the dependence of Eq. (2.23) upon the vector q, the asymmetry $\mathcal{A}$ defined by Eq. (2.20) alternates in sign in quadrants defined by the relative orientation of q with the vectors

$$\zeta_\sigma = T_{2,-1} Z_\sigma + T_{2,-2} X_\sigma \tag{2.33}$$

and

$$\chi_\sigma = \epsilon_{\mu\nu\rho\sigma} p_1^\mu p_2^\nu Q^\rho. \tag{2.34}$$

If we average the absolute value of $d\hat{\sigma}_+ - d\hat{\sigma}_-$ over the possible decay directions of the muon pair and divide by the corresponding average of $d\hat{\sigma}_+ + d\hat{\sigma}_-$, we obtain a function $\bar{\mathcal{A}}$ which depends upon two dimensionless variables, $Q^2/\hat{s}$ and $Q_\perp^2/\hat{s}$. Denoting this averaging procedure by the symbols $< \cdots >$, we define the average asymmetry $\bar{\mathcal{A}}$ by

$$\bar{\mathcal{A}} = \frac{< \Delta W >}{\left\langle \frac{1}{2}\sum_{s_1,s_2} W^{\mu\nu}(s_1,s_2) L_{\mu\nu} \right\rangle}. \tag{2.35}$$

In the rest frame of the virtual photon the vector q has components

$$q = (0, Q\sin\alpha\cos\beta, Q\sin\alpha\sin\beta, Q\cos\alpha). \tag{2.36}$$

In that frame the q dependence of ΔW can be written in the form

$$\mathbf{q}\cdot\boldsymbol{\zeta} q_y. \tag{2.37}$$

The maximum value of this expression is $Q|\zeta|/2$, but the resolution of any given detector requires one to average over some region of phase space. To get an idea of the effects of this averaging, consider an average of Eq. (2.37) over the quadrant defined by $q_y > 0, \mathbf{q}\cdot\boldsymbol{\zeta} > 0$. The result is $2Q|\zeta|/3\pi$ or $4/3\pi$ times the maximum value.

Although we will quote polarization asymmetries at the parton level to give a rough idea of asymmetries that might be expected experimentally, there are several other factors that one must consider in order to make a more precise estimate. We have computed the parton-level asymmetries by taking the ratio of the lowest-order computation of the difference and sum of the various helicity cross sections. The lowest-order results for the unpolarized cross section are known to be modified by higher-order corrections, which yield a "K factor" of order 2. This factor would reduce our estimates of the parton-level asymmetry by a corresponding factor, assuming that there is no analogous effect for the cross section difference.

The most accurate estimate of the expected experimental asymmetry would involve computing the cross section difference using the parton-level expressions given in this paper, introducing model expressions for the various parton distribution functions (introduced in Sec. V below) and accurately modeling the acceptance of the detector that is to be used in the experiment in question. An appropriate expression for the cross section sum could be taken from calculations which reproduce the K factor or from experimental data.

III. QUARK-ANTIQUARK ANNIHILATION

In this section we will discuss the process

$$q + \bar{q} \to \mu^+\mu^- + G \tag{3.1}$$

illustrated in Fig. 1. The quark carries a momentum p_1 and the antiquark momentum p_2, while the outgoing

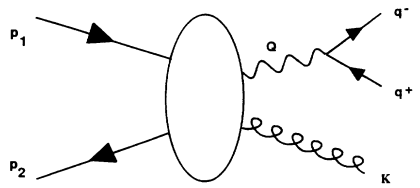

FIG. 1. Annihilation of a quark and antiquark to form a virtual photon and a gluon.

gluon has momentum K. At the tree level there are two Feynman diagrams which contribute to this process as shown in Fig. 3. For arbitrary polarization states of the initial partons, the muon pair production amplitude has the form

$$4\pi\alpha_{\rm EM}\bar{v}(p_2,s_2)\epsilon_\alpha^{(s)*}\mathcal{M}^{\mu\alpha}u(p_1,s_1) \times\frac{1}{Q^2}\bar{u}(q^-,s^-)\gamma_\mu v(q^+,s^+). \quad (3.2)$$

We have suppressed the color indices of the quark and antiquark; these indices must coincide for annihilation to take place. Neglecting quark masses, we can write the hadron tensor $W^{\mu\nu}$ as a trace in Dirac and color space

$$W^{\mu\nu}(s_1,s_2)=-\frac{1}{N^2}\mathrm{Tr}\left[\left(\frac{1-s_2\gamma_5}{2}\right)\not{p}_2\mathcal{M}^{\mu\alpha} \times\left(\frac{1+s_1\gamma_5}{2}\right)\not{p}_1\bar{\mathcal{M}}^{\nu}{}_{\alpha}\right]. \quad (3.3)$$

The factor $1/N^2$ (where N is the number of colors) refers to an average over the possible colors for the colliding quark and antiquark. This is appropriate if these partons arise from color-singlet hadrons, as we shall discuss in Sec. V of this paper. If the initial quark and antiquark are unpolarized, then at the tree level one can average over the initial quark helicities to obtain

$$\frac{1}{4}\sum_{s_1,s_2}W^{\mu\nu}(s_1,s_2)L_{\mu\nu}=\frac{N^2-1}{2N^2}(ge_i)^2\frac{2Q^2}{\hat{t}\hat{u}}[(Q^2-\hat{t})^2+(Q^2-\hat{u})^2+4(p_1\cdot q)^2+4(p_2\cdot q)^2]. \quad (3.4)$$

If one replaces the factor $W^{\mu\nu}(s_1,s_2)L_{\mu\nu}$ in Eq. (2.16) by the averaged expression, Eq. (3.4), then one obtains the muon production cross section for unpolarized quarks and antiquarks. In terms of the angles α and β Eq. (3.4) may be written as

$$\frac{1}{4}\sum_{s_1,s_2}W^{\mu\nu}(s_1,s_2)L_{\mu\nu}=\frac{N^2-1}{2N^2}(ge_i)^2\frac{2Q^2}{\hat{t}\hat{u}}\left(\hat{t}^2+\hat{u}^2+2Q^2\hat{s} +\frac{(\hat{s}^2+Q^4)(\hat{t}^2+\hat{u}^2)-4Q^2\hat{s}\hat{t}\hat{u}}{(\hat{s}-Q^2)^2}\cos^2\alpha+\frac{8Q^2\hat{s}\hat{t}\hat{u}}{(\hat{s}-Q^2)^2}\sin^2\alpha\cos^2\beta +\frac{2(\hat{u}-\hat{t})(\hat{s}+Q^2)}{(\hat{s}-Q^2)^2}\sqrt{Q^2\hat{s}\hat{t}\hat{u}}\sin 2\alpha\cos\beta\right). \quad (3.5)$$

The average value of this expression over the phase space of the muon pair produced by the virtual photon is

$$\frac{1}{4\pi}\int_0^{2\pi}d\beta\int_0^{\pi}d\alpha\sin\alpha\frac{1}{4}\sum_{s_1,s_2}W^{\mu\nu}(s_1,s_2)L_{\mu\nu} =\frac{N^2-1}{2N^2}(ge_i)^2\frac{8Q^2[(Q^2-\hat{t})^2+(Q^2-\hat{u})^2]}{3\hat{t}\hat{u}(\hat{s}-Q^2)^2}. \quad (3.6)$$

These unpolarized cross sections serve to normalize the polarized cross sections that we shall compute below.

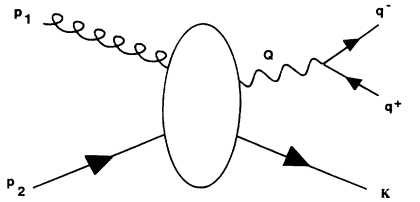

FIG. 2. Gluon scattering from a quark to produce a virtual photon.

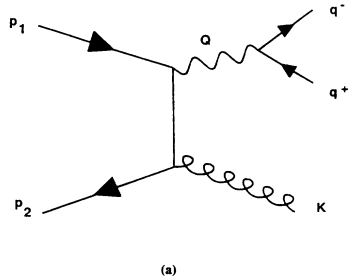

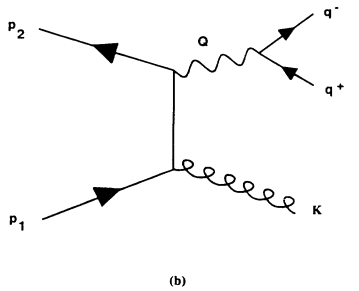

FIG. 3. Lowest-order graphs contributing to quark-antiquark annihilation.

We are interested in the cross-section difference that arises when one of the initial particles in the process (3.1), say the quark, is prepared with either positive or negative helicity and the other particle is unpolarized. Since the helicity projector is $(1 \pm \gamma_5)/2$, this cross-section difference will involve a Dirac trace with a single factor of γ_5. Note that, since all terms in $\mathcal{M}^{\mu\alpha}$ contain odd numbers of γ matrices, the helicities s_1 and s_2 must be opposite. Hence the asymmetry arising from polarized antiquarks will differ from that for polarized quarks only by a sign. The Dirac trace with one factor of γ_5 will yield an imaginary coefficient, owing to the identity

$$\mathrm{Tr}(\gamma_5 \not{a} \not{b} \not{c} \not{d}) = 4i\epsilon_{\mu\nu\rho\sigma} a^\mu b^\nu c^\rho d^\sigma . \tag{3.7}$$

Our Dirac matrix γ_5 is defined by the expression

$$\gamma_5 = i\gamma^0\gamma^1\gamma^2\gamma^3 . \tag{3.8}$$

Since the cross section difference is itself a real quantity, it follows that the amplitude $\mathcal{M}^{\mu\alpha}$ must involve a nonvanishing imaginary part to contribute. This amounts to an explicit demonstration of the time-reversal argument given in Sec. I. In the context of perturbative QCD, this observation implies that one must compute one-loop contributions to the muon pair production amplitude. These contributions are illustrated in Fig. 4. Since we are interested only in the imaginary part of these one-loop amplitudes, not all of the graphs in Fig. 4 will contribute. Given that the momenta $p_1 - Q$ and $p_2 - Q$ are spacelike, it is easy to see that graphs 4(d), 4(e), and 4(f) have no imaginary parts and need not be considered in what follows.

The real parts of the graphs in Fig. 4 contain ultraviolet divergences, but the imaginary parts are finite. Therefore it is convenient to extract the discontinuities of these graphs before evaluating the internal momentum integrals. This reduces those integrals to the form of simple and ultraviolet-convergent phase-space integrals. Individual graphs exhibit infrared divergences for massless quarks, but these divergences cancel in the observable asymmetries. We have chosen to evaluate each of these integrals in the center-of-mass frame of the particles responsible for the discontinuities and then to reexpress these results in a covariant form.

The specific discontinuities that contribute to the polarization asymmetry are shown in Fig. 5. Figure 4(a) has a nonvanishing s-channel cut, as shown in Figs. 5(1) and 5(1x). All the other graphs of Fig. 5 involve a cut through the quark and antiquark which combine to form the virtual photon. The contribution to the cross section difference from graphs 5(1) and 5(1x) must combine to yield a gauge invariant, infrared finite result—as must the contributions of the remaining graphs.

After evaluation of the phase space integrals, the contribution of any of the graphs of Fig. 5 to the polarization asymmetry may be written in terms of a quantity

$$\Delta W^{[j]} = -\frac{i}{N^2}\mathrm{Tr}[\not{p}_2 \mathrm{Im}(\mathcal{M}_\mu^{[j]\alpha})\gamma_5 \not{p}_1 \bar{\mathcal{M}}_{\nu\alpha}^{\mathrm{tree}}]L^{\mu\nu} \tag{3.9}$$

which involves the interference of an amplitude $\mathcal{M}_{\mu\alpha}^{[j]}$ with the tree amplitude $\mathcal{M}_{\nu\alpha}^{\mathrm{tree}}$ depicted in Fig. 3. If one replaces the factor $W^{\mu\nu}(s_1, s_2)L^{\mu\nu}$ in Eq. (2.16) by $\Delta W^{[j]}$, then one obtains the contribution to the difference in cross sections for positively polarized quarks and negatively polarized quarks.

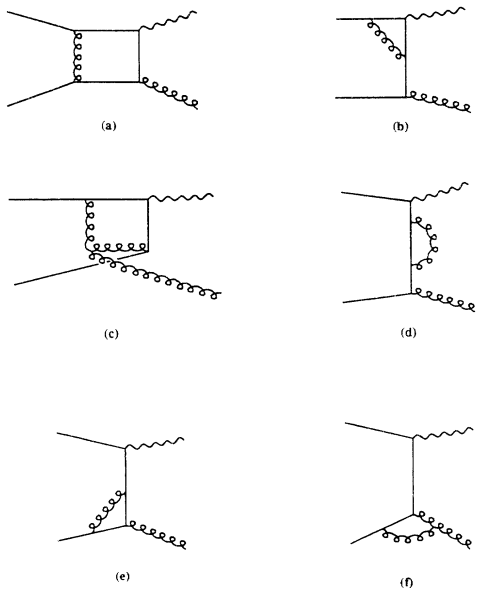

FIG. 4. One-loop corrections to the virtual photon production amplitude. Each diagram other than (c) depicts two possible processes, since each incoming line can specify either a quark or an antiquark.

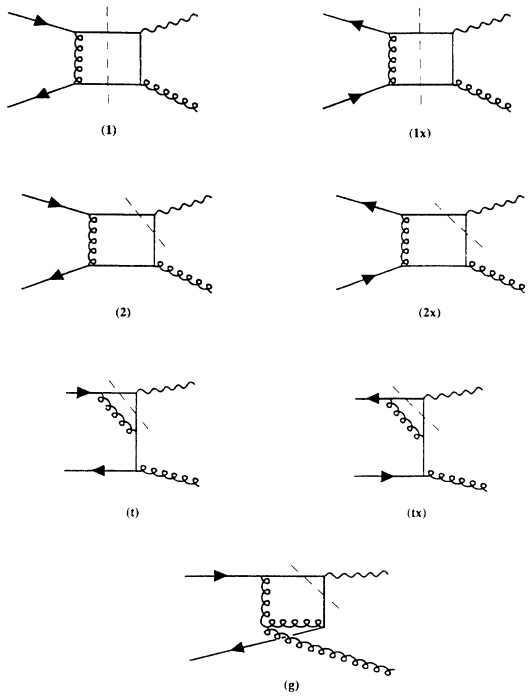

FIG. 5. Cut graphs contributing to the single-spin asymmetry.

As discussed in the preceding section, ΔW may be written in terms of two invariant functions, $T_{2,-1}$ and $T_{2,-2}$. By construction the function $T_{2,-1}$ is odd under the interchange $\hat{t} \leftrightarrow \hat{u}$, while the function $T_{2,-2}$ is even. To reduce the likelihood of algebraic error in our computations we have evaluated the momentum integrals, the transformation to relativistically invariant variables and the Dirac traces using the computer program MATHEMATICA [16]. In Appendix A we tabulate the quantities $T^{[j]}_{2,-1}$ and $T^{[j]}_{2,-2}$ and the color coefficients $C^{[j]}$ for each individual Feynman graph. If we combine graphs which correspond to the same physical discontinuity, then we obtain functions which are infrared finite, gauge invariant and physically realizable. Combining all graphs we arrive at our final results for the asymmetry associated with quark-antiquark annihilation,

$$T_{2,-1} = \frac{2Q^2(N^2-1)}{\hat{t}\hat{u}N^3}\left(\frac{(N^2-1)(Q^2+\hat{s})(\hat{u}-\hat{t})}{(Q^2-\hat{t})^2(Q^2-\hat{u})^2} - \frac{\ln[(Q^2-\hat{t})/\hat{s}]}{(Q^2-\hat{t})\hat{u}} + \frac{\ln[(Q^2-\hat{u})/\hat{s}]}{(Q^2-\hat{u})\hat{t}}\right), \tag{3.10}$$

$$T_{2,-2} = \frac{Q^2(N^2-1)}{\hat{t}\hat{u}N^3}\left[(N^2-1)\left(\frac{1}{(Q^2-\hat{t})^2}+\frac{1}{(Q^2-\hat{u})^2}\right) + 2\frac{Q^2(Q^2-\hat{s})-2\hat{t}\hat{u}}{\hat{t}\hat{u}(Q^2-\hat{t})(Q^2-\hat{u})} - \frac{2\hat{s}\ln[(Q^2-\hat{t})/\hat{s}]}{(Q^2-\hat{t})\hat{u}^2} - \frac{2\hat{s}\ln[(Q^2-\hat{u})/\hat{s}]}{(Q^2-\hat{u})\hat{t}^2}\right]. \tag{3.11}$$

In the kinematic region $-\hat{t} \ll \hat{s}$, Eqs. (3.10) and (3.11) simplify to the forms

$$T_{2,-1} \simeq \frac{2Q^2(N^2-1)^2}{N^3\hat{s}\hat{t}(Q^2-\hat{t})^2}, \tag{3.12}$$

$$T_{2,-2} \simeq \frac{-Q^2(N^2-1)^2}{N^3\hat{s}\hat{t}(Q^2-\hat{t})^2}. \tag{3.13}$$

The symmetry properties of $T_{2,-1}$ and $T_{2,-2}$ under $\hat{t} \leftrightarrow \hat{u}$ provide correspondingly simple expressions for the kinematic region $-\hat{u} \ll \hat{s}$. For fixed values of Q^2, $\hat{t}$, and $\hat{s}$, the cross section difference will depend upon the lepton momentum difference q through the factors indicated in Eq. (2.37).

Consider now the asymmetry $\mathcal{A}$ defined by Eq. (2.20). We can get an idea of the magnitude of this asymmetry if we maximize this expression over possible values of the lepton decay angles. In the limit

$$-\hat{t} \ll \hat{s}, \tag{3.14}$$

our expression for $\mathcal{A}$ is a function only of the ratio

$$\tau = -\hat{t}/Q^2 \tag{3.15}$$

and the angles which specify the orientation of the leptons. In terms of the angles α and β, the ratio $\mathcal{A}$ assumes the form

$$\mathcal{A} = \frac{N^2-1}{2N}\alpha_S \times \frac{\sqrt{\tau}\sin\alpha\sin\beta[(2+\tau)\cos\alpha - \sqrt{\tau}\sin\alpha\cos\beta]}{(1+\tau)^2(1+\cos^2\alpha)}, \tag{3.16}$$

Note that this expression vanishes in the limits $\tau \to 0$ (where there are no longer two independent transverse momenta in the final state) and $\tau \to \infty$ (where the virtual photon is massless and its decay products are necessarily collinear). If we maximize $\mathcal{A}$ with respect to these angles, we obtain the function $\mathcal{A}(\tau)$, which is plotted in Fig. 6. We see that $\mathcal{A}$ is maximal for

$$\hat{t} \simeq -0.65Q^2 \tag{3.17}$$

with a maximum value of

$$\mathcal{A}_{\max} \simeq 0.30\frac{N^2-1}{2N}\alpha_S. \tag{3.18}$$

Another indication of experimental expectations is provided by the average asymmetry $\bar{\mathcal{A}}$ of Eq. (2.35). In the limit $-\hat{t} \ll \hat{s}$, $\bar{\mathcal{A}}$ assumes the form

$$\bar{\mathcal{A}}(\tau) = \frac{N^2-1}{2N}\frac{\alpha_S}{2\pi}\sqrt{\frac{\tau(\tau+4)}{(1+\tau)^3}}. \tag{3.19}$$

This quantity is maximal for

$$\tau = \sqrt{13} - 3 \simeq 0.61, \tag{3.20}$$

where it assumes a value

$$\bar{\mathcal{A}}_{\max} \simeq 0.13\frac{N^2-1}{2N}\alpha_S. \tag{3.21}$$

The relative size of $\bar{\mathcal{A}}_{\max}$ and $\mathcal{A}_{\max}$ is roughly the factor $4/3\pi$ mentioned previously.

In the kinematic region

$$-\hat{u} \ll \hat{s}, \tag{3.22}$$

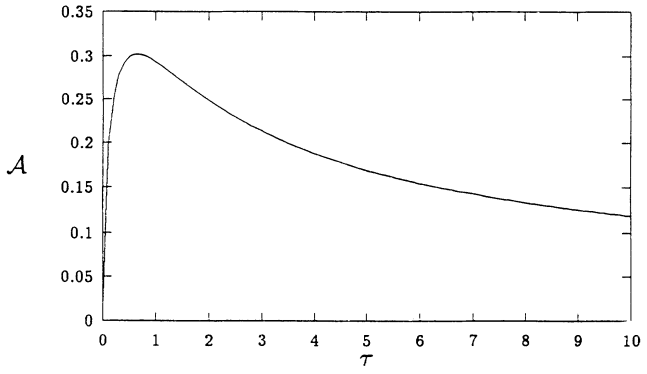

FIG. 6. Polarization asymmetry as a function of the ratio $\tau = -\hat{t}/Q^2$.

the asymmetry $\mathcal{A}$ assumes the form

$$\mathcal{A} = \frac{N^2-1}{2N}\alpha_S \times \frac{\sqrt{\omega}\sin\alpha\sin\beta[(2+\omega)\cos\alpha + \sqrt{\omega}\sin\alpha\cos\beta]}{(1+\omega)^2(1+\cos^2\alpha)}, \tag{3.23}$$

where

$$\omega = -\hat{u}/Q^2. \tag{3.24}$$

This result is essentially the same as Eq. (3.16). In particular, the maximum value of the asymmetry in this region has the same value as that given in Eq. (3.18), and the average asymmetry has the same structure as Eq. (3.19), but with the variable ω replacing τ.

Equations (3.16) and (3.23) refer to asymmetries for polarized quarks. The minus sign in the antiquark helicity projector in Eq. (3.3) implies that the cross section difference for polarized antiquarks is obtained by replacing the factor of γ_5 in Eq. (3.9) by $-\gamma_5$. Hence the sign of the cross section difference changes for the antiquark case. Note, however, that for the quark case the polarized parton is the one with momentum p_1, while for the antiquark case the polarized parton is the one with momentum p_2. This distinction will affect the sign of the result derived in Sec. V below, where we consider partons within a polarized proton.

In experiments that observe a jet recoiling against the produced muon pair, it is possible to restrict events to one of the kinematic regions specified by Eqs. (3.14) and (3.22). More generally, when one detects the muon pair and no other particles, one must integrate over a larger region of phase space. Hence we really need to know the form of the asymmetries for all values of $\hat{s}$, $\hat{t}$, and $\hat{u}$. The analytic form for these asymmetries is given by Eq. (2.35), and in Fig. 7 we display this quantity as a function of $Q^2/\hat{s}$ and $Q_\perp^2/\hat{s}$. The transverse momentum of the virtual photon is related to the other parton-level relativistic invariants by

$$Q_\perp^2 = \hat{t}\hat{u}/s. \tag{3.25}$$

The curves in Fig. 7 indicate the contours where $\bar{\mathcal{A}}$ achieves 80% of its maximum value, 60% of its maximum, etc. The numbers 80, 60, etc. label the regions where $\bar{\mathcal{A}}$ is 80–100 % of its maximum, 60–80 % of its maximum, etc. The overall maximum occurs in the lower left corner of the contour plots, where $Q^2 \ll \hat{s}$ and $Q_\perp^2 \ll \hat{s}$ and the average asymmetry takes the form (3.19).

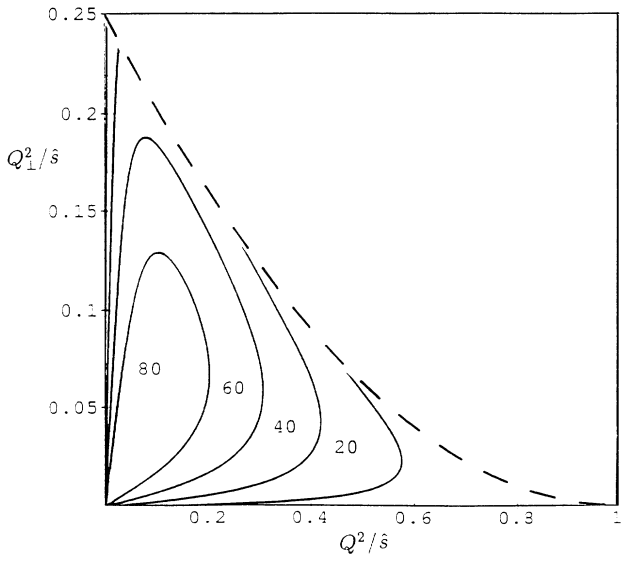

FIG. 7. Asymmetries for $q^\uparrow\bar{q}$ annihilation. Labeled regions show where the asymmetry is 80% of its maximum value, 60–80 % of maximum, etc.

IV. GLUON-QUARK SCATTERING

Let us turn now to a second source of muon pair production—the scattering of a gluon from a quark (or antiquark),

$$G + q \to \mu^+\mu^- + q, \tag{4.1}$$

illustrated in Fig. 2. The tree-level Feynman diagrams which contribute to this process are pictured in Fig. 8. For arbitrary polarizations of the gluon and quark, the muon production amplitude has the form

$$4\pi\alpha_{\rm EM}\bar{u}(K,s)\mathcal{M}^{\mu\alpha}\epsilon_\alpha^{(s_1)}u(p_2,s_2)\frac{1}{Q^2}\bar{u}(q^-,s^-)\gamma_\mu v(q^+,s^+). \tag{4.2}$$

If one does not observe the spins of the produced particles, then the cross section assumes the form of Eq. (2.16). For the scattering of massless quarks and gluons $W^{\mu\nu}(s_1,s_2)$ may be written as

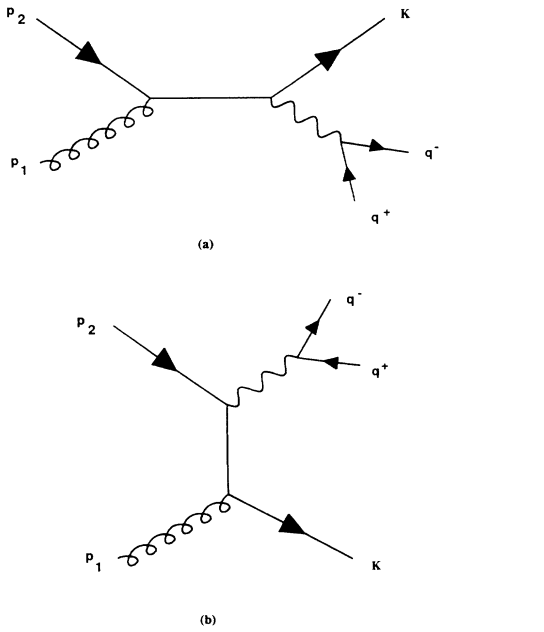

FIG. 8. Lowest-order graphs contributing to gluon-quark scattering.

$$W^{\mu\nu}(s_1,s_2)=\frac{1}{N(N^2-1)}\mathrm{Tr}\left[\not K\mathcal{M}^{\mu\alpha}\left(\frac{1+s_2\gamma_5}{2}\right)\not p_2\bar{\mathcal{M}}^{\nu\beta}\right]\epsilon_\alpha^{(s_1)}\epsilon_\beta^{(s_1)*}. \tag{4.3}$$

The factor $1/[N(N^2-1)]$ refers to an average over the color degrees of freedom for the colliding quark and gluon, which are assumed to originate from color-singlet hadrons.

At the tree level an average over the helicities and colors of the initial particles gives the expression

$$\frac{1}{4}\sum_{s_1,s_2}W^{\mu\nu}(s_1,s_2)L_{\mu\nu}=\frac{-1}{2N}(ge_i)^2\frac{2Q^2}{\hat{s}\hat{u}}[(\hat{s}-Q^2)^2+(Q^2-\hat{u})^2+4(p_2\cdot q)^2+4(K\cdot q)^2]. \tag{4.4}$$

In terms of the muon angles α and β one has

$$p_2\cdot q=\frac{Q^2\hat{t}-\hat{s}\hat{u}}{2(\hat{s}-Q^2)}\cos\alpha-\frac{\sqrt{Q^2\hat{s}\hat{t}\hat{u}}}{\hat{s}-Q^2}\sin\alpha\cos\beta, \tag{4.5}$$

$$K\cdot q=\frac{\hat{s}-Q^2}{2}\cos\alpha. \tag{4.6}$$

If one replaces the factor $W^{\mu\nu}(s_1,s_2)L_{\mu\nu}$ in Eq. (2.16) by the average value (4.4), one obtains the muon pair production cross section for unpolarized quark-gluon scattering.

We are interested in the single-spin asymmetries that result from either a longitudinally polarized quark or gluon. In either case the asymmetry must involve the imaginary part of the amplitude $\mathcal{M}_{\mu\alpha}$. If the initial quark is polarized, then the argument is the same as was given in the preceding section: the asymmetry involves a trace with a single factor of γ_5, and such a trace yields a factor of i. This factor combines with the imaginary part of $\mathcal{M}$ to yield a real contribution to the cross section difference.

The graphs that contribute at the one-loop level to muon pair production in gluon-quark collisions are shown in Figs. 9 and 10. Each of the graphs in Figs. 9 and 10 is a crossed version of one of the graphs of Fig. 4. Except for Fig. 4(c), each graph of Fig. 4 has two corresponding graphs in Figs. 9 and 10. Graphs 10(d)–10(f) have no imaginary parts in the physical region for gluon-quark scattering and need not be considered further. The specific discontinuities of the remaining graphs which do contribute to the single-spin asymmetry are shown in Figs. 11 and 12.

If the incident quark is polarized, then the contribution of the jth graph of Figs. 11 and 12 to the polarization asymmetry may be written in terms of the quantity

$$\Delta W^{[j]}=-\frac{i}{N(N^2-1)}\mathrm{Tr}[\not K\mathrm{Im}(\mathcal{M}_\mu^{[j]\alpha})\gamma_5\not p_2\bar{\mathcal{M}}_{\nu\alpha}^{\mathrm{tree}}]L^{\mu\nu}. \tag{4.7}$$

In Appendix A we tabulate the color coefficients $C^{[j]}$ and the contributions $T_{2,-1}^{[j]}$ and $T_{2,-2}^{[j]}$ for each of the graphs of Figs. 11 and 12. Combining these results, we arrive at the following functions to describe the asymmetry for polarized quarks in the gluon-quark scattering process:

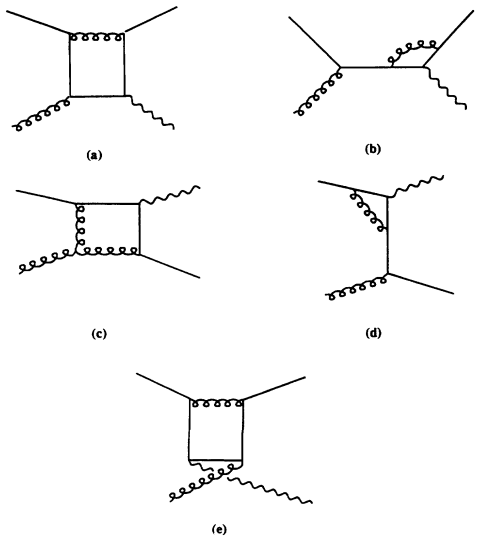

FIG. 9. A portion of the one-loop corrections to virtual photon production in gluon-quark scattering.

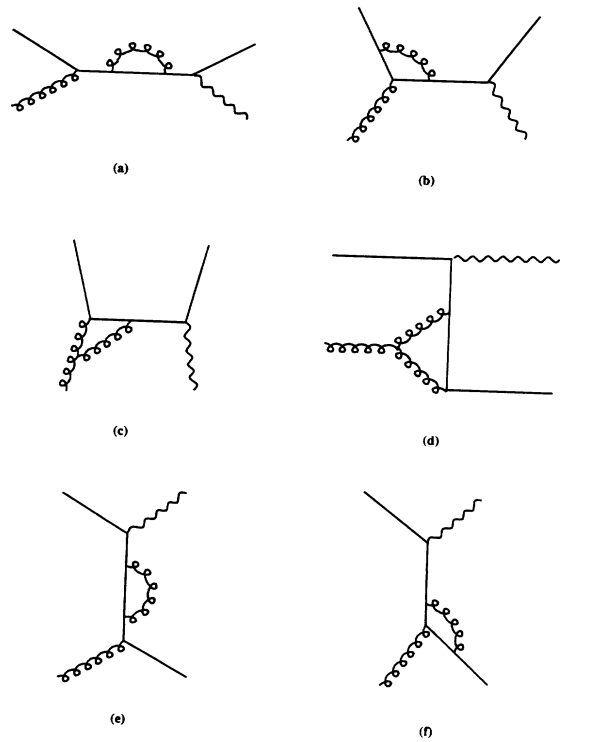

FIG. 10. The remainder of the one-loop corrections to virtual photon production in gluon-quark scattering.

$$T_{2,-1} = \frac{Q^2}{\hat{s}\hat{u}N^2}\left(\frac{(N^2-1)(\hat{u}-2\hat{t})}{(Q^2-\hat{t})(Q^2-\hat{u})^2} + 2\frac{Q^2(Q^2-\hat{t})+\hat{s}\hat{t}}{\hat{s}(Q^2-\hat{t})^2(Q^2-\hat{u})} - \frac{2\hat{t}\ln[(Q^2-\hat{t})(Q^2-\hat{u})/\hat{t}\hat{u}]}{\hat{s}^2(Q^2-\hat{u})}\right), \tag{4.8}$$

$$T_{2,-2} = \frac{Q^2}{\hat{s}\hat{u}N^2}\left(\frac{(N^2-1)(\hat{s}+2Q^2)}{(Q^2-\hat{t})(Q^2-\hat{u})^2} + 2\frac{Q^4-\hat{t}(Q^2-\hat{u})}{\hat{u}(Q^2-\hat{t})^2(Q^2-\hat{u})} - \frac{2\ln[(Q^2-\hat{t})/\hat{s}]}{\hat{u}^2} + \frac{2\ln[(Q^2-\hat{t})(Q^2-\hat{u})/\hat{t}\hat{u}]}{\hat{s}(Q^2-\hat{u})}\right). \tag{4.9}$$

Insofar as we neglect quark masses in our calculations, the corresponding result for polarized antiquarks would be the same.

Let us now consider these expressions in the kinematic region $Q_\perp^2 \ll \hat{s}$. Owing to the factor of $1/\hat{u}$ in the unpolarized cross section (2.16), this cross section is much larger for small values of $\hat{u}$ than for small $\hat{t}$. Hence we will consider the limit $-\hat{u} \ll \hat{s}$, where Eqs. (4.8) and (4.9) take the approximate form

$$T_{2,-1} \simeq \frac{2Q^2(N^2-1)}{N^2\hat{s}\hat{u}(Q^2-\hat{u})^2}, \tag{4.10}$$

$$T_{2,-2} \simeq \frac{Q^2(N^2-1)}{N^2\hat{s}\hat{u}(Q^2-\hat{u})^2}. \tag{4.11}$$

In terms of the ratio

$$\omega = -u/Q^2, \tag{4.12}$$

we obtain the following expression for the polarization asymmetry

$$\mathcal{A} = -\frac{N^2-1}{2N}\alpha_S \frac{\sqrt{\omega}\sin\alpha\sin\beta[(2+\omega)\cos\alpha + \sqrt{\omega}\sin\alpha\cos\beta]}{(1+\omega)^2(1+\cos^2\alpha)}. \tag{4.13}$$

Comparing this expression with the corresponding expression, Eq. (3.23), for the quark-antiquark annihilation process, we see that the magnitude of the single-spin asymmetry for the present process—gluon-quark scattering—is exactly the same in this kinematic region.

If one does not observe the momentum of the gluon jet, then it is not possible to restrict experimental data to lie in the region $-\hat{u} \ll \hat{s}$. Hence it is necessary to examine the structure of the asymmetry over all of phase space. Figure 13 shows the average asymmetry $\bar{\mathcal{A}}$ as a function of $Q^2/\hat{s}$ and $Q_\perp^2/\hat{s}$ throughout the region where $-\hat{t} > -\hat{u}$. The curves in Fig. 13 indicate the contours where $\bar{\mathcal{A}}$ achieves 80% of its maximum value, 60% of its maximum, etc. The numbers 80, 60, etc. label the regions where $\bar{\mathcal{A}}$ is 80–100% of its maximum, 60–80% of its maximum, etc. As in the quark-antiquark case the maximum values of the asymmetry occur for small values of $Q^2/\hat{s}$ and $Q_\perp^2/\hat{s}$, where Eq. (4.13) applies.

Let us now turn to the case where the incident gluon

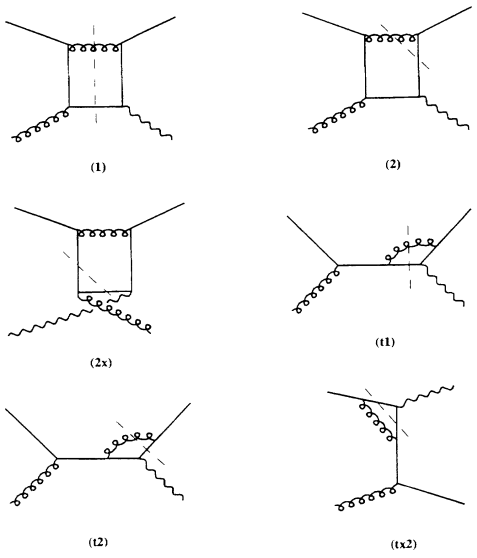

FIG. 11. A portion of the cut graphs contributing to the single-spin asymmetry for gluon-quark scattering.

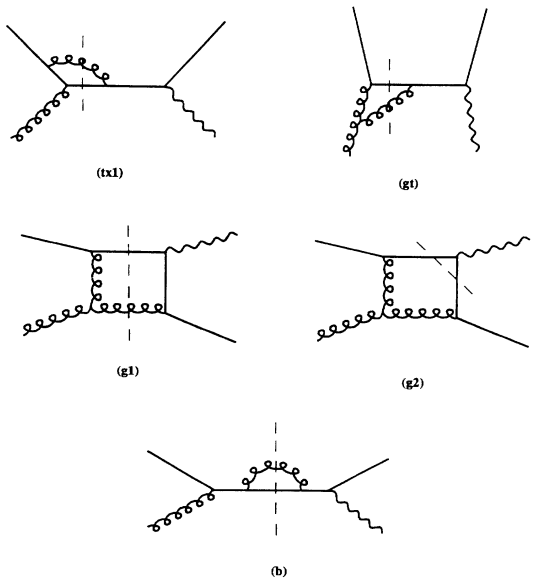

FIG. 12. The remainder of the cut graphs contributing to the single-spin asymmetry for gluon-quark scattering.

is polarized. The single-spin asymmetry in this case involves the difference

$$S_{\alpha\beta} = \epsilon_\alpha^{(1)}\epsilon_\beta^{(1)*} - \epsilon_\alpha^{(-1)}\epsilon_\beta^{(-1)*}. \tag{4.14}$$

In the center-of-mass frame we can choose

$$\epsilon^{(\pm 1)} = \frac{1}{\sqrt{2}}(0, 1, \pm i, 0) \tag{4.15}$$

so that

$$S_{\alpha\beta} = \begin{pmatrix} 0 & 0 & 0 & 0 \\ 0 & 0 & -i & 0 \\ 0 & i & 0 & 0 \\ 0 & 0 & 0 & 0 \end{pmatrix}. \tag{4.16}$$

Here again one obtains an imaginary coefficient which must combine with the imaginary part of $\mathcal{M}$ to yield a real value for the difference of cross sections with $s_i = \pm 1$. This verifies the time-reversal argument of Sec. I for this particular subprocess.

Equation (4.16) gives the form of $S_{\alpha\beta}$ in the parton center-of-momentum frame. More generally, we can write

$$S_{\alpha\beta} = \frac{2i}{\hat{s}}\epsilon_{\alpha\beta\rho\sigma}p_{1\rho}p_{2\sigma}. \tag{4.17}$$

When the initial gluon is polarized the contribution to the polarization asymmetry of the jth graph of Figs. 11 and 12 may be written as

$$\Delta W^{[j]} = \frac{i}{N(N^2-1)}\mathrm{Tr}[\not{K}\,\mathrm{Im}(\mathcal{M}_{\mu\alpha}^{[j]})\,\not{p}_2\bar{\mathcal{M}}_{\nu\beta}^{\mathrm{tree}}]L^{\mu\nu}S^{\alpha\beta}. \tag{4.18}$$

If we use Eq. (4.17) to rewrite $S_{\alpha\beta}$ in terms of the antisymmetric tensor $\epsilon_{\alpha\beta\rho\sigma}$, we can express $\Delta W^{[j]}$ in terms of invariant functions $T_{2,-1}$ and $T_{2,-2}$ exactly as in Eq. (2.23).

Appendix A gives the color factors $C^{[j]}$ for each of the graphs of Figs. 11 and 12 and their contributions to $T_{2,-1}$ and $T_{2,-2}$. The net contribution to the asymmetry for a polarized gluon scattering from an unpolarized quark is found to be

$$T_{2,-1} = \frac{Q^2}{\hat{s}\hat{u}N^2}\left(\frac{(N^2-1)(\hat{u}-2\hat{t})}{(Q^2-\hat{t})(Q^2-\hat{u})^2} + 2\frac{Q^2(Q^2-\hat{t})-\hat{s}(2\hat{s}+\hat{t})}{\hat{s}(Q^2-\hat{t})^2(Q^2-\hat{u})} - \frac{2\hat{t}\ln[(Q^2-\hat{t})(Q^2-\hat{u})/\hat{t}\hat{u}]}{\hat{s}^2(Q^2-\hat{u})}\right), \tag{4.19}$$

$$T_{2,-2} = \frac{Q^2}{\hat{s}\hat{u}N^2}\left(\frac{(N^2-1)(\hat{s}+2Q^2)}{(Q^2-\hat{t})(Q^2-\hat{u})^2} + 2\frac{Q^2(2\hat{u}-Q^2)+\hat{t}(Q^2-\hat{u})}{\hat{u}(Q^2-\hat{t})^2(Q^2-\hat{u})} + \frac{2\ln[(Q^2-\hat{t})/\hat{s}]}{\hat{u}^2} + \frac{2\ln[(Q^2-\hat{t})(Q^2-\hat{u})/\hat{t}\hat{u}]}{\hat{s}(Q^2-\hat{u})}\right). \tag{4.20}$$

The asymmetry for a polarized gluon scattering from an unpolarized antiquark would have precisely the same form insofar as we neglect quark masses in our calculations. In the limit $-\hat{u} \ll \hat{s}$, these expressions simplify to the approximate forms

$$T_{2,-1} \simeq \frac{2Q^2(N^2-1)}{N^2\hat{s}\hat{u}(Q^2-\hat{u})^2}, \tag{4.21}$$

$$T_{2,-2} \simeq \frac{Q^2(N^2-1)}{N^2\hat{s}\hat{u}(Q^2-\hat{u})^2}. \tag{4.22}$$

These results are precisely the same as those of

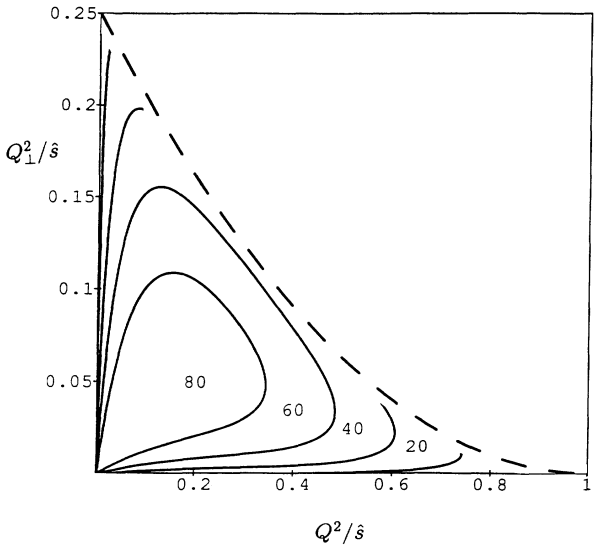

FIG. 13. Asymmetries for $q^\uparrow G$ scattering. Labeled regions show where the asymmetry is 80% of its maximum value, 60–80 % of maximum, etc.

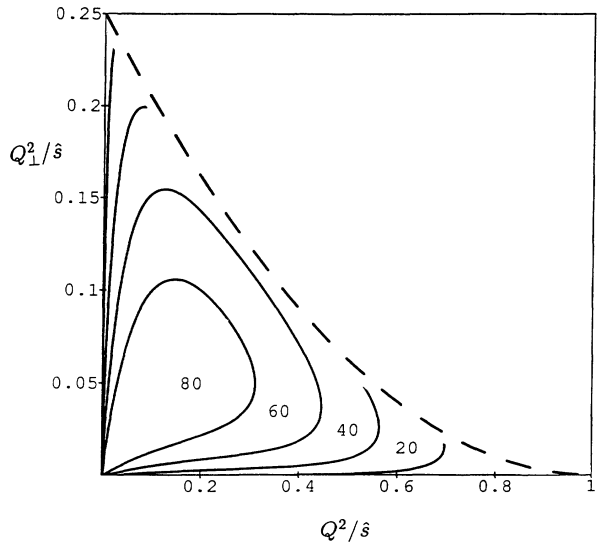

FIG. 14. Asymmetries for $G^\uparrow q$ scattering. Labeled regions show where the asymmetry is 80% of its maximum value, 60–80 % of maximum, etc.

Eqs. (4.10) and (4.11). Hence in the region $-\hat{u} \ll \hat{s}$ the polarization asymmetry for polarized gluons is identical with the result, Eq. (4.13), for polarized quarks.

Figure 14 shows the structure of the average asymmetry $\bar{A}$ in the larger region of phase space, $-\hat{u} < -\hat{t}$. The curves in Fig. 14 indicate the contours where $\bar{A}$ achieves 80% of its maximum value, 60% of its maximum, etc. The numbers 80, 60, etc. label the regions where $\bar{A}$ is 80–100 % of its maximum, 60–80 % of its maximum, etc. Once again the maximum occurs for small values of Q^2/s and $Q_\perp^2/\hat{s}$, where Eqs. (4.21) and (4.22) apply.

V. PROTON-PROTON SCATTERING

In the preceding sections we have computed single-spin asymmetries at the parton level for the production of muon pairs. In this section we discuss how to apply these results to the physical hadronic process

$$p^\uparrow + p \to \mu^+\mu^- + \text{jet} + X. \tag{5.1}$$

The kinematics for this process are illustrated in Fig. 15. If one measures the momentum K of the recoil jet, then one can fix the longitudinal momenta of the two initial partons. Therefore, if one measures the spin asymmetry for the process (5.1) and uses the theoretical expressions of Sections III and IV, one can extract information on the distribution of polarized partons within the polarized proton.

In principle, analysis of the decay products of the jet which recoils against the virtual photon could allow one to distinguish quark-antiquark annihilations from gluon-quark scattering processes. In practice, this is not easily done, and any practical experimental measurements would necessarily involve linear combinations of polarized quark, antiquark, and gluon structure functions. In this section we display the explicit combination of polarized parton distribution functions that enters a description of the process (5.1). Using known properties of the unpolarized parton distribution functions one can effectively isolate certain terms in these expressions. We will discuss this in more detail in the following section. One can also exploit the symmetry of the quark-antiquark process to eliminate it from certain linear combinations of experimental measurements. In this manner it is possible to pick out the contribution to the single-spin asymmetry of gluon-quark scattering events, even without being able to distinguish gluon and quark jets on an event by event basis.

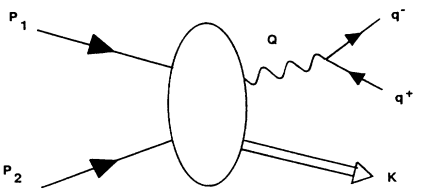

FIG. 15. Inclusive production of a muon pair and a jet in the scattering of two protons.

In this section we will assume that it is possible to resolve the kinematics of the process (5.1) completely by measuring not only the momenta of the produced muons but that of the recoil jet as well. Such measurements would allow for a detailed analysis of the process in terms of the polarized (and unpolarized) parton distribution functions. Unfortunately the practicality of such measurements is questionable. A principal virtue of muon pair production experiments lies in the possibility of filtering hadronic components out of the profusion of produced particles and concentrating on muon pairs alone. This allows one to operate the experiment at very high luminosities and effectively overcome the factor of $\alpha_{\rm EM}^2$ intrinsic to the process under consideration. If one attempts to reconstruct hadronic jets, the high event rates would become a handicap. Nonetheless it is useful to sort out the theoretical details of the process (5.1), as we shall do in this section. In the following section we will discuss the more practical experimental situation, where one does not observe the recoil jet. The expressions of the present section all apply, but one must integrate over possible values of the jet momentum. This makes it harder to extract the contribution of individual parton distribution functions to the measured single-spin asymmetry, but this can be overcome to some extent by a judicious choice of the kinematic region in which to work. Details of this discussion [14] will appear in Sec. VI.

As illustrated in Fig. 15, the momenta of the incident protons will be denoted by P_1 and P_2. The invariant momentum transferred from protons 1 or 2 to the virtual photon is given by

$$t = (P_1 - Q)^2, \tag{5.2}$$

$$u = (P_2 - Q)^2, \tag{5.3}$$

while the invariant energy is

$$s = (P_1 + P_2)^2. \tag{5.4}$$

The relation of these variables to the parton variables s, $\hat{t}$, and $\hat{u}$ introduced in Secs. III and IV will depend upon which species of partons are identified as components of protons 1 and 2. Let the momenta of these components be denoted by x_1P_1 and x_2P_2. Then the invariant energy for the parton subprocess is given by

$$s = x_1x_2s. \tag{5.5}$$

The definitions (2.6) and (2.7) specify $\hat{t}$ and $\hat{u}$ in terms of the momentum transferred from the initial quark and antiquark to the virtual photon. Hence, if a quark from proton 1 annihilates with an antiquark from proton 2, then the kinematics at the parton level are defined by

$$p_1 = x_1P_1, \tag{5.6}$$

$$p_2 = x_2P_2, \tag{5.7}$$

$$K = p_1 + p_2 - Q. \tag{5.8}$$

The parton cross section (3.4) applies with

$$t = t_* = x_1t + (1 - x_1)Q^2, \tag{5.9}$$

$$u = \hat{u}_* = x_2u + (1 - x_2)Q^2. \tag{5.10}$$

The constraint

$$\hat{s}+\hat{t}+\hat{u}=Q^2 \tag{5.11}$$

is assured by the requirement that the recoil jet be massless, i.e.,

$$\begin{aligned}K^2&=(x_1P_1+x_2P_2-Q)^2\\&=x_1(t-Q^2)+x_2(u-Q^2)+x_1x_2s+Q^2=0.\end{aligned} \tag{5.12}$$

If an antiquark from proton 1 annihilates with a quark from proton 2, the parton kinematics are defined by

$$p_1=x_2P_2, \tag{5.13}$$
$$p_2=x_1P_1, \tag{5.14}$$
$$K=p_1+p_2-Q. \tag{5.15}$$

The invariant momenta $\hat{t}$ and $\hat{u}$ which appear in Eq. (3.4) are defined by

$$\hat{t}=\hat{u}_*, \tag{5.16}$$
$$\hat{u}=\hat{t}_*. \tag{5.17}$$

For gluon-quark scattering we must consider the possibility of a quark from proton 1 interacting with a gluon from proton 2 or a quark from proton 2 interacting with a gluon from proton 1. In the first case the parton kinematics are defined by

$$p_1=x_2P_2, \tag{5.18}$$
$$p_2=x_1P_1, \tag{5.19}$$
$$K=p_1+p_2-Q. \tag{5.20}$$

The invariants $\hat{t}$ and $\hat{u}$ of Eqs. (2.6) and (2.7) are therefore given by Eqs. (5.16) and (5.17). In the second case, the parton kinematics are defined by

$$p_1=x_1P_1, \tag{5.21}$$
$$p_2=x_2P_2, \tag{5.22}$$
$$K=p_1+p_2-Q, \tag{5.23}$$

and Eqs. (5.9) and (5.10) serve to define $\hat{t}$ and $\hat{u}$.

At the parton level we have partons of momenta x_1P_1 and x_2P_2 interacting to form a muon pair with total momentum Q and a recoil jet with longitudinal momentum K^3. If one neglects the transverse momenta of the initial partons, the transverse components of K_μ are fixed to have the values

$$K_\perp=-Q_\perp. \tag{5.24}$$

The cross section at the parton level, Eq. (2.16), involves five independent variables. Two of these variables, defined as α and β in Sec. II, refer to the decay of the virtual photon. The differential cross section $K^0d\sigma/d^4Q\,d\Omega(\alpha,\beta)dK^3$ for the process (5.1) constrains the parton momentum fractions x_1 and x_2 to fixed values. These values are most easily stated in terms of the light-cone coordinates

$$p^\pm=\frac{p^0\pm p^3}{\sqrt{2}}. \tag{5.25}$$

If we neglect the proton's mass (relative to $\sqrt{s}$), then in the center-of-mass frame we have simply

$$P_1^-=P_2^+=0, \tag{5.26}$$
$$P_1^+=P_2^-=\sqrt{s/2}. \tag{5.27}$$

From Eqs. (5.2) and (5.3) it follows that

$$Q^2-t=\sqrt{2s}Q^-, \tag{5.28}$$
$$Q^2-u=\sqrt{2s}Q^+. \tag{5.29}$$

Momentum conservation at the parton level requires that

$$x_1P_1+x_2P_2=Q+K, \tag{5.30}$$

and hence

$$x_1=(Q^++K^+)/P_1^+, \tag{5.31}$$
$$x_2=(Q^-+K^-)/P_2^-. \tag{5.32}$$

The phase space for the jet and the muon pair may be conveniently written as

$$\begin{aligned}&\frac{1}{(2\pi)^5}\frac{d^3q^+}{2q_0^+}\frac{d^3q^-}{2q_0^-}\frac{d^3K}{2K^0}\delta^4(p_1+p_2-Q-K)\\&\quad=\frac{1}{4(2\pi)^5sK^0}d^4Q\,d\Omega\,dK^3\,\delta\left(x_1+x_2-\frac{2(Q^0+K^0)}{\sqrt{s}}\right)\delta\left(x_1-x_2-\frac{2(Q^3+K^3)}{\sqrt{s}}\right).\end{aligned} \tag{5.33}$$

The cross section for muon pair production from the collision of unpolarized protons may then be written in terms of parton cross sections as follows:

$$\begin{aligned}\frac{K^0d\sigma}{d^4Q\,dK^3\,d\Omega}=\frac{1}{sQ^2}\sum_i e_i^2\frac{N^2-1}{N}\Bigg(&\frac{\sigma_{q\bar{q}}}{N}[q_i(x_1)\bar{q}_i(x_2)+\bar{q}_i(x_1)q_i(x_2)]+\frac{\sigma_{qG}}{N^2-1}[q_i(x_1)+\bar{q}_i(x_1)]G(x_2)\\&+\frac{\sigma_{Gq}}{N^2-1}G(x_1)[q_i(x_2)+\bar{q}_i(x_2)]\Bigg).\end{aligned} \tag{5.34}$$

The functions $q_i(x)$, $\bar{q}_i(x)$, and $G(x)$ describe the distribution of quarks, antiquarks, and gluons in an unpolarized proton. The factors $\sigma_{q\bar{q}}$, σ_{qG}, and σ_{Gq} are given by

$$\begin{aligned}\sigma_{q\bar{q}}=\frac{\sigma_0}{\hat{t}_*\hat{u}_*}[&(Q^2-\hat{t}_*)^2+(Q^2-\hat{u}_*)^2+4x_1^2(P_1\cdot q)^2\\&+4x_2^2(P_2\cdot q)^2],\end{aligned} \tag{5.35}$$

$$\sigma_{Gq} = \frac{-\sigma_0}{\hat{s}\hat{u}_*}[\,(\hat{s}-Q^2)^2+(Q^2-\hat{u}_*)^2 +8x_2^2(P_2\cdot q)^2+4x_1^2(P_1\cdot q)^2 +8x_1x_2(P_1\cdot q)(P_2\cdot q)], \tag{5.36}$$

$$\sigma_{qG} = \frac{-\sigma_0}{\hat{s}\hat{t}_*}[\,(\hat{s}-Q^2)^2+(Q^2-\hat{t}_*)^2 +8x_1^2(P_1\cdot q)^2+4x_2^2(P_2\cdot q)^2 +8x_1x_2(P_1\cdot q)(P_2\cdot q)], \tag{5.37}$$

with

$$\sigma_0 = \frac{\alpha_S\alpha_{\rm EM}^2}{8\pi^2\hat{s}}. \tag{5.38}$$

In the kinematic region where $-t \ll \hat{s}$ and $Q^2 \ll \hat{s}$, Eq. (5.12) implies that

$$Q^+ = \frac{Q^2-u}{\sqrt{2s}} \simeq x_1\sqrt{s/2}, \tag{5.39}$$

$$Q^- = \frac{Q^2-t}{\sqrt{2s}}. \tag{5.40}$$

Similarly, one finds a large K^- for $-t \ll \hat{s}$ and a large K^+ for $-u \ll \hat{s}$. In these limits, therefore, x_1 and x_2 assume the values of the longitudinal momentum fractions of the virtual photon and jet. Specifically, for $-t \ll \hat{s}$ we have

$$x_1 \simeq x_\gamma, \tag{5.41}$$

$$x_2 \simeq x_{\rm jet} = 2|K^3|/\sqrt{s} \tag{5.42}$$

while for $-u \ll \hat{s}$

$$x_1 \simeq x_{\rm jet}, \tag{5.43}$$

$$x_2 \simeq x_\gamma. \tag{5.44}$$

In either of these limits the parton cross sections also simplify. For $-t \ll \hat{s}$ the quark-antiquark expression (5.35) assumes the form

$$\sigma_{q\bar{q}} = \sigma_0\frac{\hat{s}}{-\hat{t}_*}(1+\cos^2\alpha). \tag{5.45}$$

The corresponding expression for quark-gluon scattering, Eq. (5.37), has the same value in this limit,

$$\sigma_{qG} \simeq \sigma_{q\bar{q}}. \tag{5.46}$$

The expression for gluon-quark scattering, Eq. (5.36), is negligible in this limit, owing to the factors of $\hat{u}_*$ and $\hat{s}$ in the denominator.

It follows that in the limit $-t \ll \hat{s}$, the cross section for the muon pair production from unpolarized protons may be written as

$$\frac{d\sigma}{d^4Q\,dx_{\rm jet}\,d\Omega} = \frac{-\sigma_0\hat{s}}{sQ^2\hat{t}_*x_{\rm jet}}\sum_i e_i^2\frac{N^2-1}{N}(1+\cos^2\alpha) \times\left(\frac{1}{N}q_i(x_1)\bar{q}_i(x_2)+\frac{1}{N}\bar{q}_i(x_1)q_i(x_2)+\frac{1}{N^2-1}[q_i(x_1)+\bar{q}_i(x_1)]G(x_2)\right). \tag{5.47}$$

The functions $q_i(x)$, $\bar{q}_i(x)$, and $G(x)$ describe the distribution of quarks, antiquarks, and gluons in the unpolarized proton. In the limit $-u \ll \hat{s}$ one obtains similarly

$$\frac{d\sigma}{d^4Q\,dx_{\rm jet}\,d\Omega} = \frac{-\sigma_0\hat{s}}{sQ^2\hat{u}_*x_{\rm jet}}\sum_i e_i^2\frac{N^2-1}{N}(1+\cos^2\alpha) \times\left(\frac{1}{N}q_i(x_1)\bar{q}_i(x_2)+\frac{1}{N}\bar{q}_i(x_1)q_i(x_2)+\frac{1}{N^2-1}G(x_1)[q_i(x_2)+\bar{q}_i(x_2)]\right). \tag{5.48}$$

For the unpolarized case one cannot distinguish the two protons. For the process

$$p^\uparrow + p \to \mu^+\mu^- + \text{jet} + X \tag{5.49}$$

we denote the momentum of the polarized proton by P_1 and that of the unpolarized proton by P_2. At the parton level the cross-section asymmetry is given in terms of the product of invariant functions $T_{2,-1}$ and $T_{2,-2}$, which multiply the dot products $Z\cdot q$ and $X\cdot q$, respectively. The invariant functions depend on the parton variables $\hat{s}$, $\hat{t}$, and $\hat{u}$, which can be related to the invariant momenta at the proton level (s, t, and u) by Eq. (5.5) and either Eqs. (5.9) and (5.10) or Eqs. (5.16) and (5.17).

Where Eqs. (5.6) and (5.7) apply, the vectors Z_μ and X_μ can be written in the form

$$Z_\mu = 2x_1x_2[(P_2\cdot Q)P_{1\mu}-(P_1\cdot Q)P_{2\mu}], \tag{5.50}$$

$$X_\mu = 2x_1x_2[\,(P_2\cdot Q)P_{1\mu}+(P_1\cdot Q)P_{2\mu} -2(P_1\cdot Q)(P_2\cdot Q)Q_\mu/Q^2]. \tag{5.51}$$

Hence for the parton process

$$q^\uparrow + \bar{q} \to \mu^+\mu^- + G \tag{5.52}$$

we have

$$Z\cdot q = x_1x_2a_1, \tag{5.53}$$

$$X\cdot q = x_1x_2a_2, \tag{5.54}$$

where

$$a_1 = 2[(P_2 \cdot Q)(P_1 \cdot q) - (P_1 \cdot Q)(P_2 \cdot q)], \tag{5.55}$$

$$a_2 = 2[(P_2 \cdot Q)(P_1 \cdot q) + (P_1 \cdot Q)(P_2 \cdot q)]. \tag{5.56}$$

Similarly, for the parton process

$$\bar{q}^{\uparrow} + q \to \mu^+\mu^- + G \tag{5.57}$$

Eqs. (5.13) and (5.14) apply, and we find

$$Z \cdot q = -x_1 x_2 a_1, \tag{5.58}$$

$$X \cdot q = x_1 x_2 a_2. \tag{5.59}$$

The parton process

$$q^{\uparrow} + G \to \mu^+\mu^- + q \tag{5.60}$$

is described by the kinematics of Eq. (5.19)–(5.20). It follows that $Z \cdot q$ and $X \cdot q$ for this process are given by Eqs. (5.58) and (5.59). Finally, we have the parton process

$$G^{\uparrow} + q \to \mu^+\mu^- + q \tag{5.61}$$

with kinematics specified by Eqs. (5.22)–(5.23). The factors $Z \cdot q$ and $X \cdot q$ for this case are given by Eqs. (5.55) and (5.56).

Combining this kinematic information with the results of Secs. III and IV, we can construct the cross-section difference for muon pair production with protons of helicities $\pm\frac{1}{2}$. We define

$$\Delta\sigma = \frac{K^0 d\sigma(p^{\uparrow}p \to \mu^+\mu^- + \text{jet} + X)}{d^4Q\, d\Omega\, dK^3} - \frac{K^0 d\sigma(p^{\downarrow}p \to \mu^+\mu^- + \text{jet} + X)}{d^4Q\, d\Omega\, dK^3}. \tag{5.62}$$

Then, in terms of parton distribution functions $q(x)$ and $G(x)$ for the unpolarized proton and the corresponding functions $\Delta q(x)$ and $\Delta G(x)$ for the polarized proton, we have

$$\begin{aligned}\Delta\sigma = A\sum_i e_i^2 x_1 x_2 \{ & \Delta q_i(x_1)\bar{q}_i(x_2)[a_1 T_{2,-1}^{[q^{\uparrow}\bar{q}]}(\hat{s},\hat{t}_*,\hat{u}_*) + a_2 T_{2,-2}^{[q^{\uparrow}\bar{q}]}(\hat{s},\hat{t}_*,\hat{u}_*)] \\ & + \Delta\bar{q}_i(x_1) q_i(x_2)[-a_1 T_{2,-1}^{[\bar{q}^{\uparrow}q]}(\hat{s},\hat{u}_*,\hat{t}_*) + a_2 T_{2,-2}^{[\bar{q}^{\uparrow}q]}(\hat{s},\hat{u}_*,\hat{t}_*)] \\ & + [\Delta q_i(x_1) + \Delta\bar{q}_i(x_1)] G(x_2)[a_1 T_{2,-1}^{[q^{\uparrow}G]}(\hat{s},\hat{u}_*,\hat{t}_*) - a_2 T_{2,-2}^{[q^{\uparrow}G]}(\hat{s},\hat{u}_*,\hat{t}_*)] \\ & + \Delta G(x_1)[q_i(x_2) + \bar{q}_i(x_2)][a_1 T_{2,-1}^{[G^{\uparrow}q]}(\hat{s},\hat{t}_*,\hat{u}_*) + a_2 T_{2,-2}^{[G^{\uparrow}q]}(\hat{s},\hat{t}_*,\hat{u}_*)]\}\end{aligned} \tag{5.63}$$

with

$$A = \frac{-\alpha_S^2 \alpha_{\text{EM}}^2}{4\pi^2 s^2 Q^4} \epsilon_{\mu\nu\rho\sigma} P_1^{\mu} P_2^{\nu} Q^{\rho} q^{\sigma}. \tag{5.64}$$

Using the symmetry properties of $T^{[q^{\uparrow}\bar{q}]}$, we can write $\Delta\sigma$ in the form

$$\begin{aligned}\Delta\sigma = A\sum_i e_i^2 x_1 x_2 \{ & [\Delta q_i(x_1)\bar{q}_i(x_2) + \Delta\bar{q}_i(x_1) q_i(x_2)][a_1 T_{2,-1}^{[q^{\uparrow}\bar{q}]}(\hat{s},\hat{t}_*,\hat{u}_*) + a_2 T_{2,-2}^{[q^{\uparrow}\bar{q}]}(\hat{s},\hat{t}_*,\hat{u}_*)] \\ & + [\Delta q_i(x_1) + \Delta\bar{q}_i(x_1)] G(x_2)[a_1 T_{2,-1}^{[q^{\uparrow}G]}(\hat{s},\hat{u}_*,\hat{t}_*) - a_2 T_{2,-2}^{[q^{\uparrow}G]}(\hat{s},\hat{u}_*,\hat{t}_*)] \\ & + \Delta G(x_1)[q_i(x_2) + \bar{q}_i(x_2)][a_1 T_{2,-1}^{[G^{\uparrow}q]}(\hat{s},\hat{t}_*,\hat{u}_*) + a_2 T_{2,-2}^{[G^{\uparrow}q]}(\hat{s},\hat{t}_*,\hat{u}_*)]\}.\end{aligned} \tag{5.65}$$

In the limits $-t \ll \hat{s}$ or $-u \ll \hat{s}$ the cross-section difference simplifies. Owing to the identity

$$Q_{\perp}^2 = \frac{\hat{t}_*\hat{u}_*}{\hat{s}}, \tag{5.66}$$

one has

$$Q_{\perp}^2 \simeq -\hat{t}_* \tag{5.67}$$

for $-t \ll \hat{s}$ and

$$Q_{\perp}^2 \simeq -\hat{u}_* \tag{5.68}$$

for $-u \ll \hat{s}$. The cross-section difference $\Delta\sigma$ thus assumes the form

$$\Delta\sigma = \frac{\Delta\sigma_{\text{forward}}}{Q}{}^4 \sum_i e_i^2 \left(\frac{1}{N}[\Delta q_i(x_1)\bar{q}_i(x_2) + \Delta\bar{q}_i(x_1) q_i(x_2)] + \frac{1}{N^2-1}[\Delta q_i(x_1) G(x_2) + \Delta\bar{q}_i(x_1) G(x_2)] \right) \tag{5.69}$$

for $-t \ll \hat{s}$ and

$$\Delta\sigma = \frac{\Delta\sigma_{\text{backward}}}{Q}{}^4 \sum_i e_i^2 \left(\frac{-1}{N}[\Delta q_i(x_1)\bar{q}_i(x_2) + \Delta\bar{q}_i(x_1) q_i(x_2)] + \frac{1}{N^2-1}[\Delta G(x_1) q_i(x_2) + \Delta G(x_1)\bar{q}_i(x_2)] \right) \tag{5.70}$$

for $-u \ll \hat{s}$. The subprocess-independent part of the cross section difference is given by

$$\Delta\sigma_{\text{forward}} = \frac{-A(2a_1 - a_2)}{sQ_\perp^2}\left(\frac{N^2-1}{N}\right)^2 \frac{Q^6}{(Q^2+Q_\perp^2)^2} \tag{5.71}$$

or

$$\Delta\sigma_{\text{backward}} = \frac{-A(2a_1 + a_2)}{sQ_\perp^2}\left(\frac{N^2-1}{N}\right)^2 \frac{Q^6}{(Q^2+Q_\perp^2)^2} \tag{5.72}$$

in the respective kinematic regimes $-t \ll \hat{s}$ and $-u \ll \hat{s}$. The region $-t \ll \hat{s}$ corresponds to the production of a virtual photon moving forward along the direction of the polarized proton. Similarly, the region $-u \ll \hat{s}$ involves the production of a virtual photon moving opposite to the direction of the polarized proton (in the center-of-mass frame for the proton-proton scattering process).

Note how the symmetry of the quark-antiquark annihilation process affects the structure of the forward and backward cross-section differences: the same combination of quark and antiquark structure function, $\Delta q(x_1)\bar{q}(x_2) + \Delta\bar{q}(x_1)q(x_2)$, enters in both cases. The gluon-quark scattering process has no such symmetry. Only polarized quarks contribute to the forward production process, and only polarized gluons contribute to the backward production process. If one were to measure cross-section differences for both forward and backward production, one could extract a combination of structure functions

$$[\Delta q(x_1) + \Delta\bar{q}(x_1)]G(x_2) + \Delta G(x_1)[q(x_2) + \bar{q}(x_2)] \tag{5.73}$$

associated only with the gluon-quark scattering subprocess. In this manner one can isolate events associated with quark jets—even without having identified these jets through their decay products.

VI. EXPERIMENTAL CONSEQUENCES

In the preceding section we worked out expressions which describe the cross-section difference for muon pair production in the idealized case where one would measure the momenta of the outgoing muons and the recoil jet. We have argued that this may not be practical due to the experimental demands imposed by the constraint of jet reconstruction. In this section we consider the more realistic case [14] in which one does not observe the recoil jet. The expressions of Sec. V still apply, but one must integrate over possible values of the longitudinal momentum of the recoil jet, K^3. [The value of the jet's transverse momentum is fixed by Eq. (5.24).]

In the proton center-of-momentum frame we will let x_γ and x denote the longitudinal momentum fractions of the virtual photon and recoil jet, respectively. If the longitudinal momentum of the virtual photon follows the direction of the polarized proton, we write

$$x_\gamma = Q^+/P^+, \tag{6.1}$$
$$x = K^-/P^-. \tag{6.2}$$

If, on the other hand, the longitudinal momentum of the virtual photon follows the direction of the unpolarized proton, we write

$$x_\gamma = Q^-/P^-, \tag{6.3}$$
$$x = K^+/P^+. \tag{6.4}$$

If x_γ is large enough that the virtual photon is relativistic, then the relation between the observables x_γ and x and the parton variables x_1 and x_2 is very simple. If the virtual photon is produced in the forward direction relative to the polarized proton, then one has

$$x_\gamma = x_1, \tag{6.5}$$
$$x = x_2; \tag{6.6}$$

and if the virtual photon is produced in the backward direction relative to the polarized proton, then

$$x_\gamma = x_2, \tag{6.7}$$
$$x = x_1. \tag{6.8}$$

Both cases are of potential interest experimentally. In the first case measurement of the longitudinal momentum of the virtual photon suffices to fix the momentum fraction of the polarized parton. Hence an experiment which focuses upon this kinematic region will be able to map out the x dependence of the polarized parton distribution functions. In the second case the measured longitudinal momentum of the virtual photon fixes the momentum fraction of the unpolarized parton. This allows one to choose the value of x_γ so as to emphasize the contribution of a particular parton subprocess to the cross-section difference $\Delta\sigma$.

In either case, if one does not observe the longitudinal momentum of the recoil jet, one must integrate over possible values of x. The kinematical constraint

$$\hat{s} > Q^2 \tag{6.9}$$

fixes x to lie in the region

$$x > \frac{Q^2}{sx_\gamma}. \tag{6.10}$$

With this information we can now display the results for $\Delta\sigma$. Using Eq. (5.63) we find the following expression for a virtual photon moving forward relative to the polarized proton.

$$\begin{aligned}\Delta\sigma = A\sum_i e_i^2 x_\gamma \int_{Q^2/sx_\gamma}^1 dx\{ & [\Delta q_i(x_\gamma)\bar{q}_i(x) + \Delta\bar{q}_i(x_\gamma)q_i(x)][a_1 T_{2,-1}^{[q^\dagger\bar{q}]}(\hat{s}_*,\hat{t}_*,\hat{u}_*) + a_2 T_{2,-2}^{[q^\dagger\bar{q}]}(\hat{s}_*,\hat{t}_*,\hat{u}_*)] \\ & + [\Delta q_i(x_\gamma) + \Delta\bar{q}_i(x_\gamma)]G(x)[a_1 T_{2,-1}^{[q^\dagger G]}(\hat{s}_*,\hat{u}_*,\hat{t}_*) - a_2 T_{2,-2}^{[q^\dagger G]}(\hat{s}_*,\hat{u}_*,\hat{t}_*)] \\ & + \Delta G(x_\gamma)[q_i(x) + \bar{q}_i(x)][a_1 T_{2,-1}^{[G^\dagger q]}(\hat{s}_*,\hat{t}_*,\hat{u}_*) + a_2 T_{2,-2}^{[G^\dagger q]}(\hat{s}_*,\hat{t}_*,\hat{u}_*)]\},\end{aligned} \tag{6.11}$$

with

$$\hat{s}_* = x x_\gamma s, \tag{6.12}$$

$$\hat{t}_* = x_\gamma t + (1 - x_\gamma) Q^2, \tag{6.13}$$

$$\hat{u}_* = x u + (1 - x) Q^2. \tag{6.14}$$

The corresponding expression for a virtual photon which is produced in a direction opposite that of the polarized proton is

$$\begin{aligned}\Delta\sigma = A \sum_i e_i^2 x_\gamma \int_{Q^2/s x_\gamma}^1 dx \{ & [\Delta q_i(x)\bar{q}_i(x_\gamma) + \Delta\bar{q}_i(x) q_i(x_\gamma)][a_1 T_{2,-1}^{[q^\dagger \bar{q}]}(\hat{s}_*, \hat{t}_*, \hat{u}_*) + a_2 T_{2,-2}^{[q^\dagger \bar{q}]}(\hat{s}_*, \hat{t}_*, \hat{u}_*)] \\ & + [\Delta q_i(x) + \Delta\bar{q}_i(x)] G(x_\gamma)[a_1 T_{2,-1}^{[q^\dagger G]}(\hat{s}_*, \hat{u}_*, \hat{t}_*) - a_2 T_{2,-2}^{[q^\dagger G]}(\hat{s}_*, \hat{u}_*, \hat{t}_*)] \\ & + \Delta G(x)[q_i(x_\gamma) + \bar{q}_i(x_\gamma)][a_1 T_{2,-1}^{[G^\dagger q]}(\hat{s}_*, \hat{t}_*, \hat{u}_*) + a_2 T_{2,-2}^{[G^\dagger q]}(\hat{s}_*, \hat{t}_*, \hat{u}_*)]\},\end{aligned} \tag{6.15}$$

with

$$\hat{s}_* = x x_\gamma s, \tag{6.16}$$

$$t_* = x t + (1 - x) Q^2, \tag{6.17}$$

$$\hat{u}_* = x_\gamma u + (1 - x_\gamma) Q^2. \tag{6.18}$$

A promising application of this result has been discussed briefly in a recent paper [14]. We have suggested using either an external polarized target or an internal polarized storage cell at the Fermilab Tevatron. If one selects forward-moving events in the laboratory frame, this corresonds to a virtual photon which is moving opposite that of the polarized proton in the center-of-momentum frame (since the polarized proton in the proposed experiment is stationary in the laboratory frame). Hence Eq. (6.15) applies. By selecting events with x_γ in the range 0.2–0.4, one assures that valence quarks from the unpolarized proton should dominate. It follows that the dominant contributions in Eq. (6.15) should be those involving the combination of distribution functions $\Delta\bar{q}_i(x) q_i(x_\gamma)$ and $\Delta G(x) q_i(x_\gamma)$. Thus the proposed experiment is sensitive to a linear combination of the polarized antiquark and polarized gluon distribution functions.

If one does not detect the recoil jet, then the polarized distribution functions in Eq. (6.15) are necessarily integrated over x in a manner characteristic of inclusive muon pair production experiments. It is possible to perform an experiment which would select events in which the virtual photon is moving forward relative to the polarized proton. In such an experiment, the measured value of x_γ would correspond to the argument of the polarized distribution function, so one could map out the x dependence of these functions. To describe such an experiment one would employ Eq. (6.11), which involves an integral over the longitudinal momenta of the unpolarized quarks, so one could not select a particular subset of the contributing terms in Eq. (6.11) as we have suggested for Eq. (6.15). Furthermore, if one is using a stationary polarized target, muon pairs described by Eq. (6.15) are moving rapidly forward in the laboratory frame and are thus well-collimated. This means that a smaller detector would suffice to capture these particles efficiently. If one were working with polarized beams rather than polarized targets, the kinematic situation would be reversed, and muon pairs described by Eq. (6.11) would be the easiest to measure.

The calculations of this paper could be extended to other processes of possible experimental interest. Among the possibilities that one might consider are

$$p^\dagger + p \to \text{jet} + \text{jet} + X, \tag{6.19}$$

$$p^\dagger + p \to \gamma + \text{jet} + X. \tag{6.20}$$

Experimentally these processes are more difficult to measure, since jet reconstruction is required in each case. The two-jet process does not involve any factors of α_{EM}, so there would be no insurmountable problems with event rates for that process.

On the theoretical side both of these processes are considerably more difficult to compute than the process considered in the present paper. This is because the measured final-state particles must include two independent transverse momenta. Therefore, at the parton level one must deal with three-particle final states. In the case of Eq. (6.19) the final state involves three partons, e.g., $q + \bar{q} \to G + G + G$. In the case of Eq. (6.20) the final state would involve a photon and two partons, e.g., $q + \bar{q} \to \gamma + q + \bar{q}$. The kinematics are relatively simple, since all the particles involved are massless, but the combinatorics of a $2 \to 3$ amplitude are such as to make the computation tedious at best.

Another application of the techniques employed in the present paper might be in the investigation of single-spin asymmetries involving transversely polarized protons. Experimentally such processes are simple to measure, since one need look at only one particle in the final state. Theoretically they are more complicated to describe, since they involve operators of nonleading twist. Such operators lack a direct interpretation in terms of probabilities but may offer useful insights into the detailed structure of the proton and its proper description in the framework of QCD.

ACKNOWLEDGMENTS

In the course of this work we have profited from discussions with a number of our friends and colleagues. We would particularly like to thank Mark Strikman and Lincoln Wolfenstein for several useful observations. Our

research was supported in part by the National Science Foundation, Grant No. PHY-9024764. Final checks of the calculations in this paper were carried out while R.D.C. was a visitor at the Institute for Nuclear Theory; he would like to thank them for their kind hospitality.

APPENDIX A: CONTRIBUTIONS OF INDIVIDUAL GRAPHS

In this Appendix we provide further details of the computations described in the text. This information is given in a series of tables. Each set of tables refers to one of the three processes discussed in the text:

$$q^{\uparrow} + \bar{q} \to \mu^+\mu^- + G, \tag{A1}$$

$$q^{\uparrow} + G \to \mu^+\mu^- + q, \tag{A2}$$

$$q + G^{\uparrow} \to \mu^+\mu^- + q. \tag{A3}$$

Here the arrow ($\uparrow$) indicates which of the initial partons is polarized.

The cut graphs which contribute to the quark-antiquark annihilation process (A1) are pictured in Fig. 5. The contribution of each graph to the invariant function $T_{2,-1}$ is listed in Table I, and the contribution to $T_{2,-2}$ is given in Table II. The entries in Tables I and II do not include color factors, which are listed separately in Table III. Equations (3.10) and (3.11) give the final results for an SU(N) color theory. The corresponding results for a U(1) theory (QED) are given in terms of a decomposition of the quantity ΔW [Eq. (2.18)] in the form

$$\Delta W = -8\pi^2\alpha_{\rm EM}^2(T_{2,-1}q\cdot Z + T_{2,-2}q\cdot X)\epsilon_{\mu\nu\rho\sigma}p_1^\mu p_2^\nu Q^\rho q^\sigma. \tag{A4}$$

This decomposition replaces that of Eq. (2.23), which was appropriate for the SU(N) theory. The functions $T_{2,-1}$ and $T_{2,-2}$ for the QED case have the form

TABLE I. Invariant functions for quark-antiquark annihilation. See Fig. 5 for identification of graphs.

Graph	$\hat{t}\hat{u}T_{2,-1}$
1	$\frac{4\eta(\hat{s}+Q^2)}{(Q^2-\hat{t})(Q^2-\hat{u})} + \frac{8Q^2\ln[-\hat{t}/(\hat{s}-Q^2)]}{(Q^2-\hat{t})\hat{u}}$ $-\frac{2(Q^6-11Q^4\hat{s}+9Q^2\hat{s}^2+\hat{s}^3-4Q^4\hat{t}+12Q^2\hat{s}\hat{t}-4\hat{s}^2\hat{t})}{(Q^2-\hat{s})^2(Q^2-\hat{t})(Q^2-\hat{u})}$
1x	$\frac{-4\eta(\hat{s}+Q^2)}{(Q^2-\hat{t})(Q^2-\hat{u})} - \frac{8Q^2\ln[-\hat{u}/(\hat{s}-Q^2)]}{\hat{t}(Q^2-\hat{u})}$ $+\frac{2(Q^6-7Q^4\hat{s}+5Q^2\hat{s}^2+\hat{s}^3-4Q^4\hat{t}+4Q^2\hat{s}\hat{t}-4\hat{s}^2\hat{t})}{(Q^2-\hat{s})^2(Q^2-\hat{t})(Q^2-\hat{u})}$
2	$\frac{-8\eta Q^2}{(Q^2-\hat{t})^2} + \frac{8Q^2\ln[(Q^2-\hat{s})(Q^2-\hat{t})/\hat{s}\hat{t}]}{(Q^2-\hat{t})\hat{u}}$ $-\frac{4Q^2(Q^6+3Q^4\hat{s}-4Q^2\hat{s}^2-3Q^4\hat{t}-Q^2\hat{s}\hat{t}+2\hat{s}^2\hat{t}+2\hat{s}\hat{t}^2)}{(Q^2-\hat{s})^2(Q^2-\hat{t})^2(Q^2-\hat{u})}$
2x	$\frac{8\eta Q^2}{(Q^2-\hat{u})^2} - \frac{8Q^2\ln[(Q^2-\hat{s})(Q^2-\hat{u})/\hat{s}\hat{u}]}{\hat{t}(Q^2-\hat{u})}$ $-\frac{4Q^2(2Q^6-7Q^4\hat{s}+5Q^2\hat{s}^2-7Q^4\hat{t}+11Q^2\hat{s}\hat{t}-6\hat{s}^2\hat{t}-2\hat{s}\hat{t}^2)}{(Q^2-\hat{s})^2(Q^2-\hat{t})(Q^2-\hat{u})^2}$
t	$\frac{8\eta Q^2}{(Q^2-\hat{t})^2} - \frac{4Q^2(Q^2+2\hat{s}+3\hat{t})}{(Q^2-\hat{t})^2(Q^2-\hat{u})}$
tx	$\frac{-8\eta Q^2}{(Q^2-\hat{u})^2} + \frac{4Q^2(4Q^2-\hat{s}-7\hat{t})}{(Q^2-\hat{t})(Q^2-\hat{u})^2}$
g	$\frac{8\eta Q^2(\hat{s}+Q^2)(\hat{t}-\hat{u})}{(Q^2-\hat{t})^2(Q^2-\hat{u})^2} + \frac{8Q^2(Q^4-Q^2\hat{s}-4Q^2\hat{t}+2\hat{t}^2)}{(Q^2-\hat{t})^2(Q^2-\hat{u})^2}$

TABLE II. Invariant functions for quark-qntiquark annihilation.

Graph	$\hat{t}\hat{u}T_{2,-2}$
1	$\frac{4\eta(\hat{u}-\hat{t})}{(Q^2-\hat{t})(Q^2-\hat{u})}+\frac{8Q^2\hat{s}\ln[-\hat{t}/(\hat{s}-Q^2)]}{(Q^2-\hat{t})\hat{u}^2}-\frac{2(Q^8-10Q^6\hat{s}+10Q^4\hat{s}^2-2Q^2\hat{s}^3+\hat{s}^4-3Q^6\hat{t}+15Q^4\hat{s}\hat{t}-15Q^2\hat{s}^2\hat{t}+7\hat{s}^3\hat{t}+2Q^4\hat{t}^2-8Q^2\hat{s}\hat{t}^2+6\hat{s}^2\hat{t}^2)}{(Q^2-\hat{s})^2(Q^2-\hat{t})\hat{u}(Q^2-\hat{u})}$
1x	$\frac{4\eta(\hat{t}-\hat{u})}{(Q^2-\hat{t})(Q^2-\hat{u})}+\frac{8Q^2\hat{s}\ln[-\hat{u}/(\hat{s}-Q^2)]}{\hat{t}^2(Q^2-\hat{u})}+\frac{2(4Q^6\hat{s}-4Q^4\hat{s}^2+5Q^6\hat{t}-9Q^4\hat{s}\hat{t}+9Q^2\hat{s}^2\hat{t}-\hat{s}^3\hat{t}-2Q^4\hat{t}^2+8Q^2\hat{s}\hat{t}^2-6\hat{s}^2\hat{t}^2)}{(Q^2-\hat{s})^2(Q^2-\hat{t})\hat{t}(Q^2-\hat{u})}$
2	$\frac{8Q^2\hat{s}\ln[(Q^2-\hat{s})(Q^2-\hat{t})/\hat{s}\hat{t}]}{\hat{u}^2(Q^2-\hat{t})}-\frac{4Q^2(Q^8+3Q^4\hat{s}^2-6Q^2\hat{s}^3+2\hat{s}^4-6Q^6\hat{t}+13Q^4\hat{s}\hat{t}-15Q^2\hat{s}^2\hat{t}+6\hat{s}^3\hat{t}+7Q^4\hat{t}^2-11Q^2\hat{s}\hat{t}^2+6\hat{s}^2\hat{t}^2-2Q^2\hat{t}^3+2\hat{s}\hat{t}^3)}{(Q^2-\hat{s})^2(Q^2-\hat{t})^2\hat{u}(Q^2-\hat{u})}$
2x	$\frac{8Q^2\hat{s}\ln[(Q^2-\hat{s})(Q^2-\hat{u})/\hat{s}\hat{u}]}{\hat{t}^2(Q^2-\hat{u})}-\frac{4Q^2(2Q^6\hat{s}-2Q^4\hat{s}^2+2Q^6\hat{t}-3Q^4\hat{s}\hat{t}+3Q^2\hat{s}^2\hat{t}+Q^4\hat{t}^2+Q^2\hat{s}\hat{t}^2+2Q^2\hat{t}^3-2\hat{s}\hat{t}^3)}{(Q^2-\hat{s})^2(Q^2-\hat{t})\hat{t}(Q^2-\hat{u})^2}$
t	$-\frac{4Q^2(Q^2+\hat{s}+2\hat{t})}{(Q^2-\hat{t})^2(Q^2-\hat{u})}$
tx	$\frac{4Q^2(Q^2+\hat{s}+2\hat{t})}{(Q^2-\hat{t})(Q^2-\hat{u})^2}$
g	$\frac{8Q^2(-\hat{s}^2+Q^2\hat{t}-3\hat{s}\hat{t}-3\hat{t}^2)}{(Q^2-\hat{t})^2(Q^2-\hat{u})^2}$

TABLE III. Color factors for quark-antiquark annihilation.

Graphs	SU(N)	QED
1, 1x, 2, 2x	$-(N^2-1)/4N^3$	1
t, tx	$(N^2-1)^2/4N^3$	1
g	$-(N^2-1)/4N$	0

$$T_{2,-1}=\frac{8Q^2}{\hat{t}\hat{u}}\left(\frac{(Q^2+\hat{s})(\hat{u}-\hat{t})}{(Q^2-\hat{t})^2(Q^2-\hat{u})^2}+\frac{\ln[(Q^2-\hat{t})/\hat{s}]}{(Q^2-\hat{t})\hat{u}}-\frac{\ln[(Q^2-\hat{u})/\hat{s}]}{(Q^2-\hat{u})\hat{t}}\right), \tag{A5}$$

$$T_{2,-2}=\frac{4Q^2}{\hat{t}\hat{u}}\left(\frac{1}{(Q^2-\hat{t})^2}+\frac{1}{(Q^2-\hat{u})^2}-2\frac{Q^2(Q^2-\hat{s})-2\hat{t}\hat{u}}{\hat{t}\hat{u}(Q^2-\hat{t})(Q^2-\hat{u})}+\frac{2\hat{s}\ln[(Q^2-\hat{t})/\hat{s}]}{(Q^2-\hat{t})\hat{u}^2}+\frac{2\hat{s}\ln[(Q^2-\hat{u})/\hat{s}]}{(Q^2-\hat{u})\hat{t}^2}\right). \tag{A6}$$

Although the final results are infrared and ultraviolet finite, the contributions of the individual graphs are infrared divergent. To deal with this problem we have evaluated each graph in d space-time dimensions. Using the Dirac algebra appropriate to d dimensions, we have reduced the various traces to the form (3.7). The expressions in Tables I and II retain a formally divergent factor

$$\eta=\frac{2}{d-4}+\text{constant}, \tag{A7}$$

which cancels when one forms the physically observable differential cross sections. This cancellation provides a partial check of the validity of our calculations.

The gluon-quark scattering process (A2) is described by the entries in Tables IV–XI. The labels for the various cut graphs represented in these tables are defined by Figs. 11 and 12. Tables IV–VII describe the scattering process (A2) which involves an initially polarized quark, while Tables VIII–XI describe the case (A3) of an initially polarized gluon. The color factors associated with the graphs of Figs. 11 and 12 are given in Table XII. Combining these color factors with the entries of Tables IV–VII, one arrives at the invariant functions (4.8) and (4.9) for an SU(N) color theory. The corresponding results for QED would be

$$T_{2,-1}=\frac{4Q^2}{\hat{s}\hat{u}}\left(\frac{(\hat{u}-2\hat{t})}{(Q^2-\hat{t})(Q^2-\hat{u})^2}-2\frac{Q^2(Q^2-\hat{t})+\hat{s}\hat{t}}{\hat{s}(Q^2-\hat{t})^2(Q^2-\hat{u})}+\frac{2\hat{t}\ln[(Q^2-\hat{t})(Q^2-\hat{u})/\hat{t}\hat{u}]}{\hat{s}^2(Q^2-\hat{u})}\right), \tag{A8}$$

$$T_{2,-2}=\frac{4Q^2}{\hat{s}\hat{u}}\left(\frac{(\hat{s}+2Q^2)}{(Q^2-\hat{t})(Q^2-\hat{u})^2}-2\frac{Q^4-\hat{t}(Q^2-\hat{u})}{\hat{u}(Q^2-\hat{t})^2(Q^2-\hat{u})}+\frac{2\ln[(Q^2-\hat{t})/\hat{s}]}{\hat{u}^2}-\frac{2\ln[(Q^2-\hat{t})(Q^2-\hat{u})/\hat{t}\hat{u}]}{\hat{s}(Q^2-\hat{u})}\right). \tag{A9}$$

TABLE IV. Invariant functions for gluon-quark scattering.

Graph	Polarized quarks: $\hat{s}\hat{u}T_{2,-1}$
1	$\frac{-8\eta Q^2\hat{t}}{(Q^2-\hat{s})^2(Q^2-\hat{t})}+\frac{2(7Q^6-10Q^4\hat{s}+3Q^2\hat{s}^2-13Q^4\hat{t}+14Q^2\hat{s}\hat{t}+3\hat{s}^2\hat{t}+8Q^2\hat{t}^2+4\hat{s}\hat{t}^2)}{(Q^2-\hat{s})^2(Q^2-\hat{t})(Q^2-\hat{u})}$
2	$\frac{8\eta Q^2\hat{t}}{(Q^2-\hat{s})^2(Q^2-\hat{t})}-\frac{4Q^2(5Q^6-10Q^4\hat{s}+7Q^2\hat{s}^2-2\hat{s}^3-12Q^4\hat{t}+18Q^2\hat{s}\hat{t}-4\hat{s}^2\hat{t}+12Q^2\hat{t}^2-8\hat{s}\hat{t}^2-6\hat{t}^3)}{(Q^2-\hat{s})^2(Q^2-\hat{t})^2(Q^2-\hat{u})}$
2x	$\frac{-8\eta Q^2\hat{t}}{(Q^2-\hat{t})(Q^2-\hat{u})^2}+\frac{8Q^2\hat{t}\ln[(Q^2-\hat{t})(Q^2-\hat{u})/\hat{t}\hat{u}]}{\hat{s}^2(Q^2-\hat{u})}$ $-\frac{4Q^2(-2Q^4\hat{s}+Q^2\hat{s}^2+2\hat{s}^3+2Q^4\hat{t}+3Q^2\hat{s}\hat{t}+4\hat{s}^2\hat{t}-2Q^2\hat{t}^2+2\hat{s}\hat{t}^2)}{\hat{s}(Q^2-\hat{t})^2(Q^2-\hat{u})^2}$
g1	$\frac{2\eta(2Q^6-7Q^4\hat{s}+8Q^2\hat{s}^2-3\hat{s}^3-5Q^4\hat{t}+14Q^2\hat{s}\hat{t}-5\hat{s}^2\hat{t}+4Q^2\hat{t}^2)}{(Q^2-\hat{s})^2(Q^2-\hat{t})(Q^2-\hat{u})}$ $-\frac{4(2Q^6-4Q^4\hat{s}+2Q^2\hat{s}^2-7Q^4\hat{t}+6Q^2\hat{s}\hat{t}+3\hat{s}^2\hat{t}+4Q^2\hat{t}^2+2\hat{s}\hat{t}^2)}{(Q^2-\hat{s})^2(Q^2-\hat{t})(Q^2-\hat{u})}$

Similarly, if one combines the color factors of Table XII with the entries of Tables VIII–XI, one arrives at Eqs. (4.19) and (4.20) for the gluon-quark scattering process in an SU(N) theory with initially polarized gluons. The corresponding QED result would be

$$T_{2,-1} = \frac{4Q^2}{\hat{s}\hat{u}}\left(\frac{(\hat{u}-2\hat{t})}{(Q^2-\hat{t})(Q^2-\hat{u})^2} -2\frac{Q^2(Q^2-\hat{t})-\hat{s}(2\hat{s}+\hat{t})}{\hat{s}(Q^2-\hat{t})^2(Q^2-\hat{u})} +\frac{2\hat{t}\ln[(Q^2-\hat{t})(Q^2-\hat{u})/\hat{t}\hat{u}]}{\hat{s}^2(Q^2-\hat{u})}\right), \tag{A10}$$

$$T_{2,-2} = \frac{4Q^2}{\hat{s}\hat{u}}\left(\frac{(\hat{s}+2Q^2)}{(Q^2-\hat{t})(Q^2-\hat{u})^2} -2\frac{Q^2(2\hat{u}-Q^2)+\hat{t}(Q^2-\hat{u})}{\hat{u}(Q^2-\hat{t})^2(Q^2-\hat{u})} -\frac{2\ln[(Q^2-\hat{t})/\hat{s}]}{\hat{u}^2} -\frac{2\ln[(Q^2-\hat{t})(Q^2-\hat{u})/\hat{t}\hat{u}]}{\hat{s}(Q^2-\hat{u})}\right). \tag{A11}$$

APPENDIX B: COMPARISON WITH PREVIOUS CALCULATIONS

Previous literature [17] on the quark-antiquark process (1.6) suggested an interesting possibility with regard to measuring the polarized gluon structure function. There are two classes of partonic processes which contribute to (1.4). One involves the annihilation of a quark and antiquark to produce a gluon and a virtual photon, as illustrated in Fig. 1. The other, which is simply a crossed version of this process, involves the scattering of a gluon from a quark or antiquark to produce a virtual photon plus a quark or antiquark. This process is illustrated in Fig. 2. In Ref. [17] only the quark-antiquark annihilation process was considered, and it was argued that the resulting polarization asymmetry should be small—the consequence of a small color factor for the graphs claimed to dominate this process. The authors of Ref. [17] did not consider the gluon-quark process, since they assumed that the gluon spin fraction should be small.

Given that the gluon spin fraction might not be small, the results of Ref. [17] raised a very interesting possibility. If the contribution of the quark-antiquark process to the polarization asymmetry is small and the contribution of the gluon-quark process is not small, then measurements of the polarization asymmetry for muon pair

TABLE V. Invariant functions for gluon-quark scattering.

Graph	Polarized quarks: $\hat{s}\hat{u}T_{2,-1}$
g2	$\frac{8\eta Q^2(\hat{u}-\hat{s})\hat{t}(Q^2+\hat{t})}{(Q^2-\hat{s})^2(Q^2-\hat{t})(Q^2-\hat{u})^2} - \frac{8Q^2(2Q^6-7Q^4\hat{s}+8Q^2\hat{s}^2-3\hat{s}^3-3Q^4\hat{t}+10Q^2\hat{s}\hat{t}-8\hat{s}^2\hat{t}+4Q^2\hat{t}^2-8\hat{s}\hat{t}^2-3\hat{t}^3)}{(Q^2-\hat{s})^2(Q^2-\hat{t})(Q^2-\hat{u})^2}$
t1	$\frac{8\eta Q^2\hat{t}}{(Q^2-\hat{s})^2(Q^2-\hat{t})} - \frac{2(5Q^6-6Q^4\hat{s}-Q^2\hat{s}^2+2\hat{s}^3-11Q^4\hat{t}+10Q^2\hat{s}\hat{t}+7\hat{s}^2\hat{t}+10Q^2\hat{t}^2+4\hat{s}\hat{t}^2)}{(Q^2-\hat{s})^2(Q^2-\hat{t})(Q^2-\hat{u})}$
t2	$\frac{-8\eta Q^2\hat{t}}{(Q^2-\hat{s})^2(Q^2-\hat{t})} + \frac{4Q^2(3Q^4-5Q^2\hat{s}+2\hat{s}^2-7Q^2\hat{t}+10\hat{s}\hat{t}+7\hat{t}^2)}{(Q^2-\hat{s})^2(Q^2-\hat{t})(Q^2-\hat{u})}$
tx1	$\frac{-2}{Q^2-\hat{u}}$
tx2	$\frac{8\eta Q^2\hat{t}}{(Q^2-\hat{t})(Q^2-\hat{u})^2} - \frac{4Q^2(3Q^2-2\hat{s})}{(Q^2-\hat{t})(Q^2-\hat{u})^2}$
gt	$\frac{-2\eta(2Q^2-3\hat{s}-5\hat{t})}{(Q^2-\hat{t})(Q^2-\hat{u})} - \frac{4}{Q^2-\hat{u}}$
b	$\frac{-2(Q^2-2\hat{s}-3\hat{t})}{(Q^2-\hat{t})(Q^2-\hat{u})}$

TABLE VI. Invariant functions for gluon-quark scattering.

Graph	Polarized quarks: $\hat{s}\hat{u}T_{2,-2}$
1	$\frac{8\eta Q^4}{(Q^2-\hat{s})^2(Q^2-\hat{t})}+\frac{8Q^2\ln[-\hat{t}/(\hat{s}-Q^2)]}{\hat{u}^2}$ $+\frac{2(7Q^8-9Q^6\hat{s}-3Q^4\hat{s}^2+5Q^2\hat{s}^3-12Q^6\hat{t}+5Q^4\hat{s}\hat{t}+10Q^2\hat{s}^2\hat{t}+\hat{s}^3\hat{t}+5Q^4\hat{t}^2+6Q^2\hat{s}\hat{t}^2+\hat{s}^2\hat{t}^2)}{(Q^2-\hat{s})^2(Q^2-\hat{t})\hat{u}(Q^2-\hat{u})}$
2	$\frac{-8\eta Q^4}{(Q^2-\hat{s})^2(Q^2-\hat{t})}+\frac{8Q^2\ln[(Q^2-\hat{s})(Q^2-\hat{t})/\hat{s}\hat{t}]}{\hat{u}^2}$ $-\frac{4Q^2(5Q^8-7Q^6\hat{s}-3Q^4\hat{s}^2+7Q^2\hat{s}^3-2\hat{s}^4-9Q^6\hat{t}+4Q^4\hat{s}\hat{t}+13Q^2\hat{s}^2\hat{t}-6\hat{s}^3\hat{t}+8Q^4\hat{t}^2+2Q^2\hat{s}\hat{t}^2-6\hat{s}^2\hat{t}^2-4Q^2\hat{t}^3-2\hat{s}\hat{t}^3)}{(Q^2-\hat{s})^2(Q^2-\hat{t})^2\hat{u}(Q^2-\hat{u})}$
2x	$\frac{8\eta Q^4}{(Q^2-\hat{t})(Q^2-\hat{u})^2}-\frac{8Q^2\ln[(Q^2-\hat{t})(Q^2-\hat{u})/\hat{t}\hat{u}]}{\hat{s}(Q^2-\hat{u})}-\frac{4Q^2(2Q^4-3Q^2\hat{s}-2\hat{s}^2-3Q^2\hat{t})}{(Q^2-\hat{t})^2(Q^2-\hat{u})^2}$
g1	$\frac{2\eta(\hat{s}+Q^2)(2Q^4-7Q^2\hat{s}+3\hat{s}^2-3Q^2\hat{t}+\hat{s}\hat{t})}{(Q^2-\hat{s})^2(Q^2-\hat{t})(Q^2-\hat{u})}-\frac{4(2Q^6+2Q^4\hat{s}-6Q^2\hat{s}^2-Q^4\hat{t}-6Q^2\hat{s}\hat{t}+\hat{s}^2\hat{t})}{(Q^2-\hat{s})^2(Q^2-\hat{t})(Q^2-\hat{u})}$

TABLE VII. Invariant functions for gluon-quark scattering.

Graph	Polarized quarks: $\hat{s}\hat{u}T_{2,-2}$
g2	$\frac{8\eta Q^4(\hat{s}-\hat{u})(Q^2+\hat{t})}{(Q^2-\hat{s})^2(Q^2-\hat{t})(Q^2-\hat{u})^2}$ $+\frac{8Q^2(Q^6-2Q^4\hat{s}+3Q^2\hat{s}^2-3\hat{s}^3+Q^4\hat{t}-2Q^2\hat{s}\hat{t}-3\hat{s}^2\hat{t}-2Q^2\hat{t}^2-\hat{s}\hat{t}^2)}{(Q^2-\hat{s})^2(Q^2-\hat{t})(Q^2-\hat{u})^2}$
t1	$\frac{-8\eta Q^4}{(Q^2-\hat{s})^2(Q^2-\hat{t})}-\frac{2(5Q^6-4Q^4\hat{s}-5Q^2\hat{s}^2-2\hat{s}^3-9Q^4\hat{t}-4Q^2\hat{s}\hat{t}-\hat{s}^2\hat{t})}{(Q^2-\hat{s})^2(Q^2-\hat{t})(Q^2-\hat{u})}$
t2	$\frac{8\eta Q^4}{(Q^2-\hat{s})^2(Q^2-\hat{t})}+\frac{4Q^2(3Q^4-4Q^2\hat{s}-2\hat{s}^2-6Q^2\hat{t}-\hat{s}\hat{t})}{(Q^2-\hat{s})^2(Q^2-\hat{t})(Q^2-\hat{u})}$
tx1	$\frac{-2}{Q^2-\hat{u}}$
tx2	$\frac{-8\eta Q^4}{(Q^2-\hat{t})(Q^2-\hat{u})^2}+\frac{4Q^2(4Q^2-2\hat{s}-\hat{t})}{(Q^2-\hat{t})(Q^2-\hat{u})^2}$
gt	$\frac{-2\eta(2Q^2+3\hat{s}+\hat{t})}{(Q^2-\hat{t})(Q^2-\hat{u})}-\frac{4}{Q^2-\hat{u}}$
b	$\frac{-2(Q^2+2\hat{s}+\hat{t})}{(Q^2-\hat{t})(Q^2-\hat{u})}$

TABLE VIII. Invariant functions for gluon-quark scattering.

Graph	Polarized gluons: $\hat{s}\hat{u}T_{2,-1}$
1	$-\frac{2(-3Q^6+9Q^4\hat{s}-7Q^2\hat{s}^2+\hat{s}^3+8Q^4\hat{t}-12Q^2\hat{s}\hat{t}+2\hat{s}^2\hat{t}-2Q^2\hat{t}^2)}{(Q^2-\hat{s})^2(Q^2-\hat{t})(Q^2-\hat{u})}$
2	$-\frac{4Q^2(3Q^6-9Q^4\hat{s}+8Q^2\hat{s}^2-2\hat{s}^3-7Q^4\hat{t}+13Q^2\hat{s}\hat{t}-5\hat{s}^2\hat{t}+4Q^2\hat{t}^2-4\hat{s}\hat{t}^2-\hat{t}^3)}{(Q^2-\hat{s})^2(Q^2-\hat{t})^2(Q^2-\hat{u})}$
2x	$\frac{-8\eta Q^2\hat{t}}{(Q^2-\hat{t})(Q^2-\hat{u})^2}+\frac{8Q^2\hat{t}\ln[(Q^2-\hat{t})(Q^2-\hat{u})/\hat{t}\hat{u}]}{\hat{s}^2(Q^2-\hat{u})}-\frac{4Q^2(-2\hat{s}^3+2Q^4\hat{t}-2Q^2\hat{s}\hat{t}-3\hat{s}^2\hat{t}-2Q^2\hat{t}^2+\hat{s}\hat{t}^2)}{(Q^2-\hat{t})^2\hat{s}(Q^2-\hat{u})^2}$
g1	$\frac{4\eta(\hat{u}-\hat{t})}{(Q^2-\hat{t})(Q^2-\hat{u})}-\frac{4Q^2(Q^4-Q^2\hat{s}-Q^2\hat{t}+2\hat{s}\hat{t}+\hat{t}^2)}{(Q^2-\hat{s})^2(Q^2-\hat{t})(Q^2-\hat{u})}$
g2	$\frac{8\eta Q^2\hat{t}}{(Q^2-\hat{t})(Q^2-\hat{u})^2}-\frac{4Q^2(2Q^6-7Q^4\hat{s}+7Q^2\hat{s}^2-2\hat{s}^3-Q^4\hat{t}+2Q^2\hat{s}\hat{t}-2\hat{s}^2\hat{t}+Q^2\hat{t}^2-3\hat{s}\hat{t}^2-\hat{t}^3)}{(Q^2-\hat{s})^2(Q^2-\hat{t})(Q^2-\hat{u})^2}$

TABLE IX. Invariant functions for gluon-quark scattering.

Graph	Polarized gluons: $\hat{s}\hat{u}T_{2,-1}$
t1	$\dfrac{-2(Q^2+\hat{s})(\hat{u}-\hat{t})}{(Q^2-\hat{s})(Q^2-\hat{t})(Q^2-\hat{u})}$
t2	$\dfrac{4Q^2(\hat{u}-\hat{t})}{(Q^2-\hat{s})(Q^2-\hat{t})(Q^2-\hat{u})}$
tx1	$\dfrac{2(\hat{t}-\hat{u})}{(Q^2-\hat{t})(Q^2-\hat{u})}$
tx2	$\dfrac{8\eta Q^2\hat{t}}{(Q^2-\hat{t})(Q^2-\hat{u})^2}-\dfrac{4Q^2(Q^2-\hat{s}+3\hat{t})}{(Q^2-\hat{t})(Q^2-\hat{u})^2}$
gt	$\dfrac{4\eta(\hat{t}-\hat{u})}{(Q^2-\hat{t})(Q^2-\hat{u})}$
b	$\dfrac{2(\hat{t}-\hat{u})}{(Q^2-\hat{t})(Q^2-\hat{u})}$

production might be a particularly easy way to isolate the polarized gluon structure function. This was a prime motivation for the present work. Our new calculation of the quark-antiquark contribution fails to confirm the results of Ref. [17] in detail, but the order of magnitude of our result is the same. We find further that the quark-antiquark and gluon-quark contributions to the polarization asymmetry are comparable at the partonic level. If the polarized gluon structure function were of the same order of magnitude as the polarized antiquark structure functions, this fact would make it difficult to isolate the polarized gluon structure function experimentally, since the effects of quark-antiquark annihilation would first have to be subtracted from the measured asymmetries. But if, as may be the case, the polarized gluon structure functions are larger than the polarized antiquark structure functions, the experimental situation will be cleaner and easier to measure.

Equation (3.10) may be compared with the result of Ref. [17],

$$T_{2,-1}=\frac{2Q^2(N^2-1)}{\hat{t}\hat{u}N^3}\left(\frac{-4(Q^2+\hat{s})(\hat{u}-\hat{t})}{(\hat{t}-Q^2)^2(\hat{u}-Q^2)^2}-\frac{3(Q^2-3\hat{s})[Q^2(Q^2-\hat{s})-(\hat{t}-\hat{u})^2](\hat{u}-\hat{t})}{\hat{s}^2Q^2(\hat{s}-Q^2)(\hat{t}-Q^2)(\hat{u}-Q^2)}\right.$$
$$\left.-\frac{\ln[(Q^2-\hat{t})/\hat{s}]}{(Q^2-\hat{t})\hat{u}}+\frac{\ln[(Q^2-\hat{u})/\hat{s}]}{(Q^2-\hat{u})\hat{t}}\right) \tag{B1}$$

While the logarithms in Eqs. (3.10) and (B1) have the same form and the same coefficients, there is a discrepancy in the remaining terms. These terms appear with a color coefficient $(N^2-1)^2/N^3$ in Eq. (3.10), while in Eq. (B1) there is only a factor of $(N^2-1)/N^3$. This coefficient was emphasized by the authors of Ref. [17], as we shall discuss below. Furthermore, Eq. (B1) has a term with an analytic structure which differs from that of any of the other terms in Eq. (3.10). The denominator $\hat{s}^2Q^2(\hat{s}-Q^2)(\hat{t}-Q^2)(\hat{u}-Q^2)$ gives rise to singularities at $\hat{s}=0$, $Q^2=0$, and $\hat{s}=Q^2$. These singularities have no corresponding particles in any of the Feynman graphs of Figs. 3 or 5 and can be excluded by a direct analysis of the contributing helicity amplitudes. Suppose that we were to consider the asymmetry $\mathcal{A}'$ that would result if one used the expression (B1) of Ref. [17] and assumed that $T_{2,-2}$ were to vanish. One would have

TABLE X. Invariant functions for gluon-quark scattering.

Graph	Polarized gluons: $\hat{s}\hat{u}T_{2,-2}$
1	$\dfrac{-8Q^2\ln[-\hat{t}/(\hat{s}-Q^2)]}{\hat{u}^2}-\dfrac{2(3Q^8+8Q^6\hat{s}-6Q^2\hat{s}^3+\hat{s}^4+7Q^6\hat{t}-7Q^4\hat{s}\hat{t}-3Q^2\hat{s}^2\hat{t}+\hat{s}^3\hat{t}-4Q^4\hat{t}^2+2Q^2\hat{s}\hat{t}^2)}{(Q^2-\hat{s})^2(Q^2-\hat{t})\hat{u}(Q^2-\hat{u})}$
2	$\dfrac{-8Q^2\ln[(Q^2-\hat{s})(Q^2-\hat{t})/\hat{s}\hat{t}]}{\hat{u}^2}$ $-\dfrac{4Q^2(3Q^8-11Q^6\hat{s}+10Q^4\hat{s}^2-2Q^2\hat{s}^3-9Q^6\hat{t}+19Q^4\hat{s}\hat{t}-10Q^2\hat{s}^2\hat{t}+\hat{s}^3\hat{t}+8Q^4\hat{t}^2-10Q^2\hat{s}\hat{t}^2+2\hat{s}^2\hat{t}^2-2Q^2\hat{t}^3+\hat{s}\hat{t}^3)}{(Q^2-\hat{s})^2(Q^2-\hat{t})^2\hat{u}(Q^2-\hat{u})}$
2x	$\dfrac{8\eta Q^4}{(Q^2-\hat{t})(Q^2-\hat{u})^2}-\dfrac{8Q^2\ln[(Q^2-\hat{t})(Q^2-\hat{u})/\hat{t}\hat{u}]}{\hat{s}(Q^2-\hat{u})}-\dfrac{4Q^2(2Q^4-2Q^2\hat{s}-2Q^2\hat{t}+3\hat{s}\hat{t}+\hat{t}^2)}{(Q^2-\hat{t})^2(Q^2-\hat{u})^2}$
g1	$\dfrac{4\eta(Q^2+\hat{s})}{(Q^2-\hat{t})(Q^2-\hat{u})}-\dfrac{4Q^2(Q^4-2Q^2\hat{s}-2Q^2\hat{t}+\hat{s}\hat{t})}{(Q^2-\hat{s})^2(Q^2-\hat{t})(Q^2-\hat{u})}$

TABLE XI. Invariant functions for gluon-quark scattering.

Graph	Polarized gluons: $\hat{s}\hat{u}T_{2,-2}$
g2	$\frac{-8\eta Q^4}{(Q^2-\hat{t})(Q^2-\hat{u})^2}+\frac{4Q^2(2Q^6-5Q^4\hat{s}+4Q^2\hat{s}^2-2\hat{s}^3+Q^4\hat{t}-4Q^2\hat{s}\hat{t}+\hat{s}^2\hat{t}-2Q^2\hat{t}^2+\hat{s}\hat{t}^2)}{(Q^2-\hat{s})^2(Q^2-\hat{t})(Q^2-\hat{u})^2}$
t1	$\frac{-2(Q^2+\hat{s})^2}{(Q^2-\hat{s})(Q^2-\hat{t})(Q^2-\hat{u})}$
t2	$\frac{4Q^2(Q^2+\hat{s})}{(Q^2-\hat{s})(Q^2-\hat{t})(Q^2-\hat{u})}$
tx1	$\frac{-2(\hat{s}+Q^2)}{(Q^2-\hat{t})(Q^2-\hat{u})}$
tx2	$\frac{-8\eta Q^4}{(Q^2-\hat{t})(Q^2-\hat{u})^2}+\frac{4Q^2(4Q^2-\hat{s})}{(Q^2-\hat{t})(Q^2-\hat{u})^2}$
gt	$\frac{-4\eta(\hat{s}+Q^2)}{(Q^2-\hat{t})(Q^2-\hat{u})}$
b	$\frac{-2(\hat{s}+Q^2)}{(Q^2-\hat{t})(Q^2-\hat{u})}$

$$\mathcal{A}'=\frac{-\alpha_S}{4N}\frac{\sqrt{\tau}\sin\alpha\sin\beta[(\tau+2)(\tau+3)\cos\alpha-2(5+\tau)\sqrt{\tau}\sin\alpha\cos\beta]}{(1+\tau)^2(1+\cos^2\alpha)}. \tag{B2}$$

In the limit $\tau\to\infty$ this expression grows indefinitely—a consequence of the factor of Q^2 in the denominator of the second term of Eq. (B1). This is an unphysical result.

Because of the discrepancy between our results and those of Ref. [17] we performed a second, independent calculation of the quark-antiquark process. Our second approach employed the spinor helicity method [18], which simplifies the computation to the extent that one can compute all of the contributing Feynman graphs by hand. We verified that these manual calculations agreed with our machine results quoted in Sec. III. We will reserve details of this approach for a separate publication, where we will also perform a check of the quark-gluon processes considered in the present paper.

TABLE XII. Color factors for gluon-quark scattering.

Graphs	SU(N)	QED
1, 2, 2x, tx1	$-1/4N^2$	1
b, t1, t2, tx2	$(N^2-1)/4N^2$	1
g1, g2, gt	$-1/4$	0

The authors of Ref. [17] did not compute the function $T_{2,-2}$, arguing that it would be relatively unimportant in the kinematic region

$$Q_\perp^2\ll\hat{s} \tag{B3}$$

where the unpolarized cross section (3.4) is largest. In terms of relativisitic invariants one can write

$$\hat{s}Q_\perp^2=\hat{t}\hat{u} \tag{B4}$$

or

$$\hat{s}(Q_\perp^2+Q^2)=(Q^2-\hat{t})(Q^2-\hat{u}). \tag{B5}$$

Hence the region (B3) corresponds to

$$-\hat{t}\ll\hat{s} \tag{B6}$$

or

$$-\hat{u}\ll\hat{s}. \tag{B7}$$

Inspection of Eqs. (3.10) and (3.11) shows that $T_{2,-1}$ and $T_{2,-2}$ are of the same order of magnitude in this region.

Owing largely to the form of the color factor Eq. (B1),

the authors of Ref. [17] argued that the polarization asymmetry associated with quark-antiquark annihilation should be very small. This observation formed part of the motivation for the present work, since a process in which the quark-antiquark contribution to the polarization asymmetry would be small might be a process in which it is particularly easy to extract the structure functions for polarized gluons. Since our results differ considerably from those of Ref. [17], we have had to reconsider their analysis completely.

[1] G. Baum *et al.*, Phys. Rev. Lett. **38**, 673 (1977).
[2] EM Collaboration, J. Ashman *et al.*, Phys. Lett. B **206**, 364 (1988); Nucl. Phys. **B328**, 1 (1989).
[3] J. Ellis and R.L. Jaffe, Phys. Rev. D **9**, 1444 (1974).
[4] R.D. Carlitz and J. Kaur, Phys. Rev. Lett. **38**, 673 (1977).
[5] A.V. Efremov and O.V. Teryaev, JINR Report No. E2-88-287, 1988 (unpublished); G. Altarelli and G.G. Ross, Phys. Lett. B **212**, 391 (1988); R.D. Carlitz, J.C. Collins, and A.M. Mueller, *ibid.* **214**, 229 (1988).
[6] J. Ellis and M. Karliner, Phys. Lett. B **213**, 73 (1988); G. Preparata, P.G. Ratcliffe, and J. Soffer, Phys. Rev. Lett. **61**, 1167 (1990); F.E. Close, *ibid.* **64**, 361 (1990); G. Preparata, P.G. Ratcliffe, and J. Soffer, *ibid.* **64**, 495 (1990).
[7] E. Berger and J. Qiu, Phys. Rev. D **40**, 778 (1989).
[8] M.B. Einhorn and J. Soffer, Nucl. Phys. **B274**, 714 (1986).
[9] J.C. Collins and J. Kwiecinski, Nucl. Phys. **B316**, 307 (1989).
[10] G. Altarelli and G. Parisi, Nucl. Phys. **B126**, 298 (1977).
[11] R.D. Carlitz, J.C. Collins, and A.M. Mueller, in *New Results in Hadronic Interactions*, Proceedings of the 24th Rencontre de Moriond, Les Arcs, France, 1989, edited by J. Tran Thanh Van (Editions Frontières, Gif-sur-Yvette, 1989).
[12] C. Bourrely, J. Soffer, F.M. Renard, and P. Taxil, Phys. Rep. **117**, 319 (1989); J.Ph. Guillet, in *Polarized Collider Workshop*, edited by J.C. Collins, S.F. Heppelman, and R.W. Robinett, AIP Conf. Proc. No. 223 (AIP, New York, 1991).
[13] R. Gilman *et al.*, Phys. Rev. Lett. **65**, 1733 (1990).
[14] R.D. Carlitz and R.S. Willey, University of Pittsburgh Report No. 91-10 (unpublished).
[15] J.P. Ralston and D.E. Soper, Nucl. Phys., **B152**, 109 (1979).
[16] S. Wolfram, *Mathematica* (Addison-Wesley, Reading, MA, 1991).
[17] B. Pire and J.P. Ralston, Phys. Rev. D **28**, 260 (1983).
[18] Z. Xu, D-H. Zhang, and L. Chang, Nucl. Phys. **B291**, 392 (1987).